ALDH1A1 overexpression in melanoma cells promotes tumor angiogenesis by activating the IL-8/Notch signaling cascade

VALERIO CICCONE[1], ERIKA TERZUOLI[1], EMMA RISTORI[1,2], ARIANNA FILIPPELLI[1], MARINA ZICHE[3], LUCIA MORBIDELLI[1] and SANDRA DONNINI[1]

[1]Department of Life Sciences, University of Siena, Siena I-53100, Italy; [2]Yale Cardiovascular Research Center, Department of Internal Medicine, Yale University School of Medicine, New Haven, CT 06511, USA; [3]Department of Medicine, Surgery and Neurosciences, University of Siena, Siena I-53100, Italy

Received February 12, 2022; Accepted April 29, 2022

DOI: 10.3892/ijmm.2022.5155

Abstract. ALDH1A1 is a cytosolic enzyme upregulated in tumor cells, involved in detoxifying cells from reactive aldehydes and in acquiring resistance to chemotherapeutic drugs. Its expression correlates with poor clinical outcomes in a number of cancers, including melanoma. The present study hypothesized that the increased ALDH1A1 expression and activity upregulated the release of proangiogenic factors from melanoma cells, which regulate angiogenic features in endothelial cells (ECs) through a rearrangement of the Notch pathway. *In vivo*, when subcutaneously implanted in immunodeficient mice, ALDH1A1 overexpressing melanoma cells displayed a higher microvessel density. In a 3D multicellular system, obtained co-culturing melanoma cancer cells with stromal cells, including ECs, melanoma ALDH1A1 overexpression induced the recruitment of ECs into the core of the tumorspheres. By using a genes array, overexpression of ALDH1A1 in tumor cells also promoted modulation of Notch cascade gene expression in ECs, suggesting an interaction between tumor cells and ECs mediated by enrichment of angiogenic factors in the tumor microenvironment. To confirm this hypothesis, inactivation of ALDH1A1 by the pharmacological inhibitor CM037 significantly affected the release of angiogenic factors, including IL-8, from melanoma cells. High levels of ALDH1A1, through the retinoic acid pathway, regulated the activation of NF-κB-p65 and IL-8. Further, in a 2D co-culture system, the addition of an IL-8 neutralizing antibody to ECs co-cultured with melanoma cells forced to express ALDH1A1 dampened endothelial angiogenic features, both at the molecular (in terms of gene and protein expression of mediators of the Notch pathway) and at the functional level (proliferation, scratch assay, tube formation and permeability). In conclusion, these findings demonstrated the existence of a link between melanoma ALDH1A1 expression and EC Notch signaling modification that results in a pro-angiogenic phenotype. Based on the crucial role of ALDH1A1 in melanoma control of the tumor microenvironment, the enzyme seems a promising target for the development of novel drugs able to interrupt the cross-talk between cancer (stem) cells and endothelial cells.

Correspondence to: Professor Sandra Donnini, Department of Life Sciences, University of Siena, 2 Via Aldo Moro, Siena I-53100, Italy
E-mail: sandra.donnini@unisi.it

Key words: aldehyde dehydrogenase 1A1, IL-8, melanoma, stemness, angiogenesis, Notch, multicellular 3D system

Introduction

Cutaneous melanoma is a lethal form of skin cancer with an incidence that has been rapidly increasing in the past decades. Melanoma has high metastatic potential and shows therapy resistance, resulting in extremely poor prognosis for this disease (1,2). The development of checkpoint inhibitors (anti-programmed death protein 1, anti-programmed death ligand 1 and anti-cytotoxic T-lymphocyte antigen-4) and targeted therapy with B-Raf (BRAF) and mitogen-activated protein kinase kinase (MEK) nhibitors have revolutionized the treatment of metastatic melanoma, but a number of patients eventually develop progressive disease (3). The understanding of melanoma pathogenesis is crucial for the development of new therapeutic strategies.

Numerous studies have demonstrated that tumor progression and resistance to therapies are driven by the close interplay among tumor microenvironment (TME) cells and genetic lesions and plasticity of cancer cells (4-6). In particular, the communication between tumor cells and the bystander endothelial cells (ECs) is essential in regulating angiogenesis and instrumental for the spread of metastasis (7). The interaction between tumor cells and cells of TME can be direct or indirect through the secretion of soluble factors, cytokines and chemokines and extracellular cell-matrix remodeling (8). IL-8 is a well-known pro-inflammatory and pro-angiogenic chemokine that is prominently expressed in immune, endothelial and tumor cells (9). The effect of IL-8 signaling has received considerable attention as a key modulator in the context of TME (10).

During tumor progression, cancer cells must adapt to changes in TME conditions, such as mechanical stress, altered oxygen tension and nutrient availability (10,11).

Reactive oxygen species (ROS) overproduction in TME causes oxidation of polyunsaturated fatty acids in the cellular membrane of cancer cells through free radical chain reactions with the formation of aldehydes as final products, which serve a crucial role in the pathogenesis and progression of cancer (12). Aldehyde dehydrogenases (ALDHs), a family of NADP-dependent enzymes involved in the detoxification of endogenous/exogenous aldehydes, are proposed as a marker of cancer stem cells in several types of cancer, including melanoma, non-small cell lung cancer (NSCLC), gastric and breast tumors (13-15). Furthermore, some ALDHs, particularly aldehyde dehydrogenase 1A1 (ALDH1A1), 1A3 (ALDH1A3) and 3A1 (ALDH3A1) are associated with cell self-protection, differentiation, expansion, tumor progression and therapy resistance (16). Building on this evidence, the authors have previously demonstrated the contribution of ALDH1A1 in tumor angiogenesis in pre-clinical breast cancer models (17) and the role of ALDH3A1 in promoting stem cell development, epithelial-mesenchymal transition and immune evasion in melanoma and NSCLC cell lines (18).

In light of the emerging complexities related to ALDHs influence on cancer phenotype and shaping of TME, the present study investigated the link between ALDH1A1 expression in melanoma cells and the acquisition of pro-angiogenic phenotype of normal endothelium in *in vivo* xenografts and in 2D and 3D co-culture models, focusing on tumor and endothelial components of the TME.

The present study demonstrated that ALDH1A1 activity and expression in melanoma cells regulated angiogenesis features in endothelium via the production and release of IL-8 and, in turn, the modulation of the gene expression profile of the Notch signaling pathway.

Materials and methods

Chemicals and reagents. The ALDH1A1 inhibitor CM037 was from ChemDiv Inc. CM037 was dissolved in DMSO (10 mM). CelLytic MT Cell Lysis Reagent, goat serum and Eukitt quick-hardening mounting medium for microscopy, 3 kDa FITC-Dextran, ARA-C and DAPI were from Merck KGaA. Fluoromount aqueous mounting medium was from Thermo Fisher Scientific, Inc. Lentiviral particles were from OriGene Technologies, Inc. Matrix Matrigel (growth factors and phenol red-free) was from Becton Dickinson. Anti-IL-8 antibody from R&D Systems (cat. no. MAB208). Tissue-Tek O.C.T. was from Sakura. Retinoic acid and pan-RAR antagonist (cat. no. AGN 193109) were from Tocris Bioscience.

Cell culture. Melanoma cells A375, metastatic human melanoma cells WM-266-4 (passages 5-20; ATCC), immortalized human keratinocytes HaCaT (Voden Medical, SpA) and normal human dermal fibroblasts NHDF (Lonza Group, Ltd.) were cultured in DMEM 4500 high glucose (Euroclone, SpA) supplemented with 10% fetal bovine serum (FBS; HyClone; Cytiva) and 2 mM glutamine, 100 units penicillin and 0.1 mg/l streptomycin (Merck KGaA). Cells were propagated by splitting 1:6 twice a week for A375, WM-266-4 and HaCaT and 1:3 twice a week for NHDF.

Human umbilical vein endothelial cells (HUVECs) were purchased from PromoCell GmbH. They were grown in endothelial growth medium (EGM-2), containing vascular endothelial growth factor (VEGF), recombinant human long R3 insulin like growth factor 1 (R3-IGF-1), human epidermal growth factor (hEGF), human fibroblastic growth factor (hFGF), hydrocortisone, ascorbic acid, heparin and GA-1000 (Lonza Group, Ltd.), 10% FBS and 2 mM glutamine, 100 units/ml penicillin and 0.1 mg/ml streptomycin (Merck KGaA). HaCaT cells authentication was by STR profiling.

To create GFP-HUVECS, the third generation of lentiviral particles was used. GFP-HUVECS were kindly provided by Professor Ambra Grolla, University of Piemonte Orientale A. Avogadro, Novara, Italy. Cells were cultured at 37˚C in 5% CO_2.

To achieve a stable knockdown, $1.5x10^5$ melanoma cells were seeded on 6-multiplates and transduced at 70% confluence with lentiviral particles (Merck KGaA) carrying a scrambled (SC; pLKO.1-puro Empty Vector Control Transduction Particles also from Merck KGaA) or two ALDH1A1 short hairpin (sh)RNA sequences (TRC N 0000276459 and TRC N 0000276397) and expressing the puromycin-resistant gene (ALDH1A1KD). A MOI (Multiplicity of Infection) of 10 was used. The cells were incubated at 37˚C. At 36 h post-infection, puromycin (2 μg/ml) was added to cells and selection was allowed for 3 days. Stable knockdown was validated by western blot. Cells were used in the experiments or split for propagation. Selected cells were maintained in complete medium with puromycin (1 μg/ml).

The sequence of plasmid inserted in cells clone 1 (ShA) was: 5'-CCGGCACCGATTT-GAAGATTCAATACTCGA GTATTGAATCTTCAAATCGGTGTTTTTG.

The sequence of plasmid inserted in cells clone 2 (ShB) was: 5'-CCGGCTCTAGCTTTGTCATAGTTATCTCGAGAT AACTATGACAAAGCTAGAG-TTTTTG.

To generate stable ALDH1A1 overexpressed ($ALDH1A1^+$) cultures, $1.5x10^5$ melanoma cells were seeded on 6-multiplates and infected with lentiviral particles containing nucleotide sequences encoding for ALDH1A1 (Origene RC200723 LentiORF particles, ALDH1A1 (Myc-DDK tagged) - Human). The empty vector for overexpression was from OriGene Technologies, Inc. (cat. no. PS100001). A MOI of 10 was used. The cells were incubated at 37˚C. At 36 h post-infection, medium was replaced with complete culture medium containing G418 (400 μg/ml). $ALDH1A1^+$ cells were generated by G418 selection for 10 days. Stable overexpression was validated by western blot. Cells were used in the experiments or split for propagation. Selected cells were maintained in a complete medium with G418 (400 μg/ml).

The clones were expanded and used until 20 passages.

In vivo tumor xenograft. The present study was conducted in accordance with the ethical standards and according to the Declaration of Helsinki and the Italian law (Legislative Decree no.26, 4 March 2014), which acknowledges the European Directive 2010/63/UE, being approved by the animal welfare board of University of Siena and the Italian Ministry of Health (authorization n. 62/2014-B). To assess the involvement of ALDH1A1 in tumor growth and angiogenesis, immunodeficient mice (5 week-old female athymic mice, 20-25 g, Envigo) were subcutaneously (s.c.) inoculated in the right flank with $1x10^7$ A375 cells/100 μl (50 μl of cells and 50 μl of Matrigel).

The mice were kept in temperature- and humidity-controlled rooms (22˚C and 50%) with a 12-h light/dark cycle and water and food available *ad libitum*. A total of 18 different mice were randomly assigned to three different groups of six mice. In the first group, mice were injected with A375 ALDH1A1SC. A375 ALDH1A1KD and A375 ALDH1A1^{+} were injected respectively in the second and third group. Mice were observed daily. No side effects such as changes in body weight, behavioral changes or other signs of discomfort were observed. The duration of experiment was 23 days, a coherent time to study tumor angiogenesis. At the end of the experiment the animals were euthanized by carbonic dioxide inhalation. The volume displacement for euthanasia of the animals was 30-70% vol/min. Death was ascertained by respiratory arrest. Each tumor was embedded in Tissue-Tek O.C.T., cooled in isopentane and frozen in liquid nitrogen for histology.

Immunofluorescence staining on O.C.T. sections. Cryostat sections (7 μm) from tissue samples were used for immunofluorescence staining with anti-CD31 antibody. Sections were rehydrated with PBS and fixed with 4% paraformaldehyde for 20 min at room temperature. Subsequently, sections were washed and permeabilized with 0.2% Triton-X100 in PBS for 20 min. After the washes (3x5 min) with PBS, sections were blocked with 5% goat serum in PBS at room temperature. Samples were incubated for 18 h (at 4˚C) with anti-CD31 (BD Biosciences, cat. no: 550274) in 5% goat serum in PBS (dilution 1:100). After washes (3x5 min) with PBS, secondary antibody (goat anti-rat Alexa Fluor 568) in 5% goat serum in PBS (dilution 1:200) were applied for 60 min in the dark at room temperature. Samples were washed (3x5 min) with PBS and incubated with DAPI in PBS (1:5,000). Sections were washed (3x5 min) with PBS and mounted in Eukitt. Quantification of CD31 positive vessels was performed counting by fluorescence microscope (Nikon Eclipse TE 300) five random fields for section, each slide having five sections (magnification, x20). Analysis was performed by GraphPad Prism 7 (GraphPad Software, Inc.).

In vitro multicellular skin spheroid and melanoma tumorspheres. Commercially available cell lines were mixed as described to recreate *in vitro* multicellular skin and melanoma tumorspheres (19,20). For multicellular 3D skin spheroids, HaCaT, NHDF and HUVECs were mixed in equal proportions (1x10^{3} cells each). To create multicellular melanoma 3D tumorspheres A375 (SC, ALDH1A1KD or ALDH1A1^{+}) were cultured with HaCaT, NHDF and HUVECs (1x10^{3} cells each). All tumorspheres were seeded in ultralow attachment plates (Corning, Inc.) and grown in endothelial growth medium (EGM-2), containing VEGF, R3-IGF-1, hEGF, hFGF, hydrocortisone, ascorbic acid, heparin and GA-1000 (Lonza Group, Ltd.), 10% FBS, 2 mM glutamine, 100 units/ml penicillin and 0.1 mg/ml streptomycin (Merck KGaA). Tumorspheres were cultured at 37˚C in 5% CO_2 for 6 days. At the end of experiment tumorspheres were analyzed with a confocal microscope (Zeiss LSM700; Zeiss GmbH).

Tumorspheres fluorescence analyses. 3D tumorspheres were harvested and fixed in 4% paraformaldehyde for 18 h at 4˚C as previously reported (21) after three washes with PBS, tumorspheres were permeabilized with 0.2% Triton-X100 in PBS for 20 min at room temperature and then nuclei were labeled with DAPI (1:5,000 for 10 min at room temperature). Spheroids were washed (3x5 min) with PBS and mounted in Fluoromount aqueous mounting medium. Images were captured using Nikon Eclipse TE 300 (Nikon Corporation; magnification, x20).

GFP-HUVECS sorting. To isolate GFP-HUVECS from melanoma 3D tumorspheres, spheroids were harvested and trypsinized with 5 mM EDTA and 2.5% trypsin at room temperature. Cells were centrifuged (5 min at 4˚C and 300 x g) and resuspended in PBS. GFP-HUVECS were then isolated by using BD FACSAria Fusion (BD Biosciences).

RNA isolation and reverse transcription-quantitative (RT-q) PCR. Total RNA was prepared using RNeasy Plus kit (cat. no. 74134 Qiagen GmbH) following the manufacturer's instructions. The quality and quantity of the purified RNA were redetermined by measuring the absorbance at 260/280 nm (A260/A280) using Infinite F200 Pro, (Tecan Group, Ltd.). A total of 500 ng (for GFP-HUVECS) or 1 μg (for tumor cells) of RNA were reverse transcribed using QuantiTect Reverse Transcription kit (cat. no. 205313 Qiagen GmbH; 42˚C for 30 min and the reaction was then terminated by incubating the tube at 95˚C for 3 min).

RT-qPCR was performed using QuantiNova SYBR Green PCR kit (cat. no. 208056 Qiagen GmbH) in a RotorGene qPCR machine (Qiagen GmbH) under the following conditions: 95˚C for 5 min, followed by 45 cycles of 95˚C for 20 sec, 60˚C for 20 sec and then at 72˚C for 20 sec.

Fold change expression was determined by the comparative Ct method (ΔCt) normalized to 60S ribosomal protein L19 expression. RT-qPCR data were represented as Ct value (cycle threshold) or fold increase relative to GFP-HUVECS from melanoma tumorspheres ALDH1A1SC or ALDH1A1KD, assigned to 1 (22).

The primer sequences were: *DLL4* forward, 5'-AATGGA GGCAGCTGTAAGGA-3' and reverse, 5'-CATAGTAGC CCGGAGGACAC-3'; *NOTCH1* forward, 5'-GGCAATCCG AGGACTATGAG-3' and reverse, 5'-CAGAACGCACTC GTTGATGT-3'; *NOTCH3* forward, 5'-AGGCCATGGTCT TCCCTTAC-3' and reverse, 5'-TCAATCTCCAGCATTACT ACCG-3'; *ADAM17* forward, 5'-AACAGCGACTGCACG TTGAAGG-3' and reverse, 5'-CTGTGCAGTAGGACACGC CTTT-3'; *Bcl-2* forward 5'-TTGTGGCCTTCTTTGAGT TCGGTG-3' and reverse 5'-GGTGCCGGTTCAGGTACT CAGTCA-3'; *Bax* forward 5'-CCTGTGCACCAAGGTGCC GGAACT-3' and reverse 5'-CCACCCTGGTCTTGGATC CAGCCC-3'; *IL-8* forward, 5'-GAGCACTCCATAAGG CACAAA-3' and reverse 5'-ATGGTTCCTTCCGGTGGT-3'; *RPL19* forward 5'-GATGCCGGAAAAACACCTTG-3' and reverse 5'-TGGCTGTACCCTTCCGCTT-3'. All primers were from Merck KGaA.

Proliferation of HUVECs in co-culture with melanoma cells. TME communication between melanoma and ECs was reconstructed *in vitro* using a Transwell system (Corning, Inc.) (17). Transwells provide 2D-co-culture without contact between two cell types. HUVECs (5x10^{3} cells) were seeded

on the bottom of 24 multiplates precoated with gelatin. Melanoma cells were plated on the polyester membrane of the Transwell ($2x10^4$ cells). After 24 h, tumor cells were pre-treated for 1 h with CM037 (10 μM; in DMEM with 1% FBS, 37˚C) and then co-cultured with HUVECs in the same 24 multiplates for 48 h in the presence of EBM medium (without growth factors) with 1% FBS. Anti-IL-8 neutralizing antibody was added at 80 ng/ml, where appropriate. Cells were then fixed using Fixing for fast staining (methanol based) (Panoptic No. 1) for 15 min at room temperature and then stained using Eosin for fast staining (Panoptic No. 2) and Blue for fast staining (Panoptic No. 3; Azur B based; 15 min each; PanReac AppliChem). Cells were randomly counted at original magnification of x20 in five fields as previously reported (17). Analysis was performed by GraphPad Prism 7 (GraphPad Software, Inc.).

Scratch assay in HUVECs co-cultured with melanoma cells. HUVECs ($1x10^5$ cells) were seeded on the bottom of 12-well multiplates pre-coated with gelatin. Once HUVECs reached confluence, cells were scratched using a sterile 100-1,000 μl micropipette tip to create a wound ±500 μm across the monolayer and Transwells were put in the same 12-well multiplates for 18 h of co-culture in EBM medium (without growth factors, but with 1% FBS). ARA-C (2.5 μg/ml) was then added to all the wells to control cell proliferation. Where appropriate, tumor cells were pre-treated for 1 h (at 37˚C) with CM037 (10 μM) and then co-cultured with HUVECs (at 37˚C) as described above. Where indicated, co-culture was treated with the neutralizing anti-IL-8 antibody at 80 ng/ml. Images of the wound in each well were acquired from 0-18 h under a phase contrast microscope (Nikon Eclipse TE 300, Nikon), at x20 magnification. The rate of scratch area was measured by quantifying the uncovered area of the wound that HUVECs covered starting from the edge of the scratch. All quantifications were done with Fiji software (64-bit Java 1.8.0_172). Results are expressed as a percentage of the area of the wound at 18 h respect to time 0 (23). Analysis was performed by GraphPad Prism 7 (GraphPad Software, Inc.).

Permeability assay in HUVECs co-cultured with melanoma cells. Permeability assay was performed in endothelial monolayers as previously described (17). Briefly, melanoma (SC, ALDH1A1KD and ALDH1A1$^+$) were seeded at a density of $3x10^4$ on the bottom of 12-well multiplates. HUVECs ($8x10^4$ cells) were seeded on the top of the polycarbonate membrane with 0.4 μm pores, pre-coated with gelatin. After 24 h incubation necessary for cell adherence, Transwells were put in the same 12-well multi-plates with medium supplemented with 1% FBS until HUVECs confluence (at 37˚C). Anti-IL-8 anti-body was added, where indicated, at 80 ng/ml. Fluorescein isothiocyanate-dextran (FITC-Dextran, 3 kDa; added at 10 μM concentration in the upper compartment of the Transwell, at 37˚C) was used as a fluorescent marker of paracellular permeability, which was evaluated after 15 min by measuring the fluorescence of medium in the lower compartment in a multi-plate reader (Infinite F200 Pro; Tecan Group, Ltd.) at 485 and 535 nm excitation and emission, respectively. Data are reported as fluorescence units.

Tube formation assay by HUVECs co-cultured with melanoma cells. Tumor cells ($3x10^4$ cells) were cultured on Transwell inserts. After 24 h the inserts were transferred on top of HUVECs plated on Matrigel ($1.5x10^5$ cells in 12-well multiplates) at 37˚C. Where appropriate, tumor cells were pre-treated for 1 h with CM037 (10 μM) and then co-cultured with HUVEC. Anti-IL-8 antibody was added at 80 ng/ml.

After 18 h of incubation (at 37˚C), images of the ECs were captured and network formation on Matrigel was quantified by using Fiji Software using the number of branching points under a light microscope (five random fields/well; Nikon Eclipse E400 and camera Nikon DS5MC; Nikon Corporation) at magnification x20 (24).

Human cytokine ELISA plate array. Human Cytokine ELISA Plate Array (cat. no. EA-4001, Signosis, Inc.) was performed for quantitative comparison of 31 cytokines on supernatants of melanoma cells treated with CM037 (a selective ALDH1A1 enzyme blocker). Cells ($3x10^3$) were exposed to a medium with 1% FBS in the presence/absence of CM037 (1 μM) for 48 h (with CM037 treatment every 24 h). The cell culture supernatants from each sample were incubated for 2 h at room temperature in the wells of the cytokine ELISA plate and the captured cytokine proteins were subsequently detected with a cocktail of biotinylated detection antibodies against 31 human cytokines The test sample was allowed to react with a pair of antibodies, resulting in the cytokines being sandwiched between the solid phase and enzyme-linked antibodies. After incubation at room temperature (2 h), the wells were washed to remove unbound-labeled antibodies. The plate was further detected with horseradish peroxidase (HRP) luminescent substrate (cat. no. EA-4001; Signosis, Inc.). The level of expression for each specific cytokine is directly proportional to the luminescence intensity. Data were reported as percentage of fold change vs. untreated cells (Ctr). The experiment was performed twice in duplicate.

Human Notch signaling real time-based array analysis. The human Notch signaling RT Profiler PCR array (PAHS-059Y, Qiagen GmbH) was used to profile a panel of 84 genes representative of the Notch pathway in HUVECs co-cultured with A375 cells (A375 ALDH1A1SC, ALDH1A1KD and ALDH1A1$^+$) for 6 days at 37˚C. HUVECs were seeded on the bottom of 6-well multiplates ($8x10^4$ cells) and tumor cells on the top of the Transwell ($5x10^4$ cells). The medium was changed every two days.

RNA was isolated from HUVECs using a RNeasy Plus kit at room temperature (cat. no. 74134 Qiagen GmbH) and then reverse transcribed using QuantiTect Reverse Transcription kit (cat. no. 205313 Qiagen GmbH; 42˚C for 30 min and the reaction was then terminated by incubating the tube at 95˚C for 3 min). The cDNA was used on the real-time RT Profiler PCR array (PAHS-059Y, Qiagen GmbH). The experiment was performed twice.

Western blotting. Western blotting was performed on HUVECs co-cultured with A375 cells for 6 days at 37˚C. HUVECs ($1.5x10^5$ cells) were seeded on the bottom of 6-well multiplates pre-coated with gelatin. A375 cells were plated on

the polyester membrane of the Transwell ($8x10^4$ cells). After 24 h, tumor cells were co-incubated with ECs in the same 6-well multiplates for 6 days in the presence of EBM medium (without growth factors) with 1% FBS. Where indicated, co-cultures were treated with the neutralizing anti-IL-8 antibody at 80 ng/ml (the treatment was repeated every 48 h). Melanoma cells ($3x10^5$) were seeded in 60 mm Petri dishes. After adherence, cells were starved for 4 h and then treated with retinoic acid (1 μM, 24 h) or 2% FBS for 24 h at 37˚C. Proteins were isolated and western blotting were performed as previously described. Proteins were isolated and western blotting were performed as previously described (25). After collecting the cells, proteins were extracted using CelLytic MT supplemented with 2 mM Na_3VO_4 and 1X Protease inhibitor cocktail for mammalian cells (Merck KGaA). The protein concentration was measured using a Bradford assay. Proteins (50 μg) were separated by polyacrylamide gel electrophoresis (Bolt 4 to 12%, Bis-Tris, 1.0 mm, Mini Protein Gel, 10-well, from Thermo Fisher Scientific, Inc.) and then transferred onto a nitrocellulose membrane (iBlot 2 Transfer Stacks, nitrocellulose, regular size from Thermo Fisher Scientific, Inc.). After blocking with 5 % nonfat dried milk (1 h at room temperature) (cat. no. 1706404; Bio-Rad Laboratories, Inc.), the membranes were incubated at 4˚C overnight with primary antibody including: anti-ALDH1A1 (rabbit, 1:1,000, cat. no. 54135), anti- delta-like canonical Notch ligand 4 (Dll4; rabbit, 1:1,000, cat. no. 2589), anti-Notch1 (rabbit, 1:1,000, cat. no. 3608), anti-recombining binding protein, suppressor of hairless (RBPSUH; rabbit, 1:1,000, cat. no. 5313) and anti-A disintegrin and metalloproteinase-17 (ADAM17; rabbit, 1:1,000, cat. no. 6978) antibodies were from Cell Signaling Technology, Inc. Anti-β-actin antibody (mouse, 1:10,000, cat. no. MABT825) was from Merck KGaA. Anti-NF-κB p65 (rabbit, 1:1,000, cat. no. sc-8008) was from Santa Cruz Biotechnology, Inc. The membranes were than incubated with secondary antibodies IgG (H+L), HRP conjugate (anti-rabbit, 1:2,500, cat. no. W401B; anti-mouse 1:2,500, cat. no. W402B, both from Promega Corporation) at room temperature for 1 h and washed with PBS and Tween20 0.5 % three times. Protein bands were analyzed by ChemiDoc XRS (Bio-Rad Laboratories, Inc.) following incubation at room temperature for 2 min with enhanced chemiluminescent substrate (Euroclone SpA).

ALDH1A1 enzymatic activity. ALDH1A1 enzymatic activity was determined by measuring the conversion of acetaldehyde to acetic acid, as previously reported (17). Briefly, cells were scraped into 600 μl lysis buffer (100 mM Tris-HCl pH 8.0, 10 mM DTT, 20% glycerol, 1% Triton X-100) and centrifuged at 16,000 x g for 20 min at 4˚C. The supernatant was used to detect ALDH activity at 25˚C by monitoring NADH formation from NAD+ at 340 nm in a spectrophotometer (Infinite F200 Pro; Tecan Group, Ltd.). The assay mixture (0.8 ml) contained 100 mM sodium pyrophosphate pH 9.0, 10 mM NAD+ and 600 μg of sample protein. The reaction was initiated by adding acetaldehyde (10 mM) to the cuvette. The enzyme-specific activity was expressed as nmol NADH/minute/mg protein.

MTT assay. Cell survival was quantified by MTT (Thiazolyl Blue Tetrazolium Bromide, Sigma Aldrich) (26). Briefly, cells ($3x10^3$) were seeded in 96-multiwell plates in medium with 10% serum for 24 h and then grown for 48 h in complete medium with 10% FBS at 37˚C in the presence or not of CM037 (1-10 μM) every 24 h. Dimethyl sulfoxide (DMSO) was used to dissolve the formazan salt. Data are reported as absorbance measured at 540 nm/well.

Immunofluorescence analysis. NF-κB p65 (anti-rabbit; 1:50; cat. no. sc-8008; Santa Cruz Biotechnology, Inc.) localization was monitored by fluorescence microscope. A total of $3x10^4$ A375 (ALDH1A1SC, ALDH1A1KD and ALDH1A1$^+$) were seeded on 1-cm circular glass coverslips. After 24 h incubation at 37˚C, cells were starved for 4 h and then treated with retinoic acid (1 μM, for 1 h) or DMEM supplemented with 2% FBS at 37˚C. Immunofluorescence analysis was performed on ECs as previously reported (17). Briefly, the cells were fixed at room temperature with cold acetone for 15 min and washed three times with PBS. After blocking with 5% goat serum (at room temperature) for 1 h, the cells were incubated with primary antibody diluted with goat serum and incubated at 4˚C for 18 h. After three washes with PBS, secondary antibody was added (goat anti-rat Alexa Fluor 488) for 1 h at room temperature in the dark. Cells were washed with PBS and incubated with DAPI (1:5,000 at room temperature for 20 min). After washing, they were mounted on specimen slides.

HUVECs proliferation. A total of 1,000 cells/well (of a 96-well multiplate) were left to adhere in an incubator at 37˚C in 10% serum for 24 h and then IL-8 (used at increasing concentrations in the range 0.1-100 ng/ml) was added in a medium with 1% serum which represented the basal control condition. All experimental points using cells from the single culture plate were run in triplicate. After 48 h, cells were fixed using 100% Fixing for fast staining (Panoptic No. 1) for 15 min at room temperature and then stained using Eosin for fast staining (Panoptic No. 2) and Blue for fast staining (Panoptic No. 3; 15 min each) and randomly counted under a light microscope x20 original magnification in five fields. Data are reported as number of cells counted/well.

Data analysis and statistical procedures. Results are either representative or the average of at ≤3 independent experiments performed in triplicate. Statistical analysis was performed using one-way ANOVA test followed by the Bonferroni test and the unpaired Student t-test when appropriate (GraphPad Prism 7; GraphPad Software, Inc.). $P<0.05$ was considered to indicate a statistically significant difference.

Results

Melanoma ALDH1A1 promotes angiogenic recruitment and Notch signaling modulation in vivo and in a model of 3D tumor spheroids. Intrinsic ALDH1A1 serves an important role in the stemness and progression of several solid tumors, including melanoma (27). Since tumor progression is closely related to the crosstalk that tumor cells establish with the TME components, the present study investigated the phenotype of ECs in terms of angiogenic functions and remodulation of gene expression when exposed to melanoma cells expressing ALDH1A1. The present study employed the following cell

lines: A375 mutated BRAF(V600E) and WM-266-4 metastatic BRAF wild type melanoma cells. To strengthen the contribution of melanoma ALDH1A1 in regulating the pro-angiogenic phenotype of ECs, we used loss- and gain-of-function strategies. The present study created cellular models knocked down for ALDH1A1 (ALDH1A1KD clones sh A and B) in A375 and WM-266-4 cells. For gain-of function cells, A375 ALDH1A1$^+$ and WM-266-4 ALDH1A1$^+$ cells were generated. Melanoma cells infected with a scrambled sequence were reported as ALDH1A1SC cells and used as control. As expected, compared with ALDH1A1SC melanoma cells, ALDH1A1KD melanoma cells showed a reduction of ALDH1A1 protein expression (Fig. 1A and B) and impairment of enzyme function, evaluated by ALDH1A1 enzymatic activity assay (Fig. 1C and D). By contrast, A375 ALDH1A1$^+$ and WM-266-4 ALDH1A1$^+$ melanoma cells demonstrated increased ALDH1A1 activity (Fig. 1C and D) and expression (Fig. 1E and F).

It was determined whether the reduced expression and activity of ALDH1A1 in melanoma cancer cells influenced *in vivo* tumor angiogenesis. A375 ALDH1A1KD, A375 ALDH1A1$^+$ and A375ALDH1A1SC were implanted s.c. in nude mice and the density of angiogenic microcapillaries in A375 tumors evaluated. By immunostaining for CD31, a significant increase of vessels in ALDH1A1$^+$ tumors was found compared with ALDH1A1KD ones (Fig. 1G and H).

To investigate the contribution of the concerted interactions of melanoma multiple cell components on ECs phenotype, multicellular melanoma 3D tumorspheres were developed with close contacts among different cell types (19,20). The present study focused in particular on the communication of tumor cells and ECs and how melanoma cells expressing different levels of ALDH1A1 enzyme 'corrupt' normal ECs. A375 (ALDH1A1SC, ALDH1A1KD and ALDH1A1$^+$) were seeded with keratinocytes HaCat, dermal fibroblasts NHDF and GFP-HUVECS in equal proportions to generate multicellular melanoma 3D tumorspheres. As a control, a model of skin spheroids (HaCat, NHDF and GFP-HUVECS) was used. Spheroids were grown for 6 days to favor cell-cell interaction and matrix deposition to obtain multicellular structurally established spheroids. Fig. 1I and J show that the skin spheroids presented a circular shape with regular and homogeneous edges. Instead, multicellular melanoma tumorspheres had an irregular shape, were more aggregated and presented a less homogeneous structure (Fig. 1I and J). The dimension and number of ALDH1A1$^+$ tumorspheres were higher in respect of ALDHKD and skins spheroids (Fig. 1I).

Focusing on tumor angiogenesis, the recruitment of GFP-HUVECS in skin 3D spheroids and multicellular melanoma tumorspheres was determined. Fluorescence analysis showed the presence of a cluster of GFP-HUVECS in the central region of the tumorspheres (Fig. 1K). The multicellular melanoma tumorspheres showed more significant infiltration of GFP-HUVECS compared with skin spheroids. Among the tumorspheres, A375 ALDH1A1KD tumorspheres displayed the lowest ability to recruit ECs. On the other hand, the Z-stacks analysis on confocal microscopy images revealed a 3D organization of endothelium in multicellular A375 ALDH1A1$^+$ tumorspheres, showing vessel-like tubule structures of green ECs with bifurcation (Fig. 1L). Whether tumor cells harboring different levels of ALDH1A1 might influence canonical angiogenesis pathways in ECs was then investigated, focusing on Notch signaling, which is known to contribute to vascular development and remodeling (28-30). First, to investigate whether co-culture of HUVECs in 3D organization with tumor cells affected HUVECs viability, qPCR analysis was performed to study apoptosis-related genes. The Bax/Bcl-2 ratio was analyzed. As shown in Fig. S1, compared with HUVECs grown in monolayer, no differences in the Bax/Bcl-2 ratio were observed. Then, the Notch signaling pathway in GFP-HUVECS sorted by BD FACSAria Fusion from A375 ALDH1A1KD, A375 ALDH1A1$^+$ and ALDH1A1SC tumorspheres was investigated. RT-qPCR analysis of these cells revealed an increase of DLL4 gene transcription in endothelium derived from A375 ALDH1A1$^+$ 3D tumorspheres compared with HUVECs recovered from A375 ALDH1A1SC (Fig. 1M) and A375 ALDH1A1KD 3D spheres (Fig. 1N). An increased expression was observed for DLL4, NOTCH1 and ADAM17 transcripts, exclusively in HUVECs derived from A375 ALDH1A1$^+$ compared with A375 ALDH1A1KD 3D tumorspheres (Fig. 1N).

These results indicated that tumor ALDH1A1 levels correlated with angiogenic phenotype and increased microvessel density *in vivo*. In TME *in vitro* settings, a genetic modulation of Notch signaling in ECs was observed, suggesting an enrichment of angiogenic factors in the TME driven by melanoma ALDH1A1.

ALDH1A1 expression and activity in melanoma cells regulate IL-8 release and control ECs proliferation, migration, tube formation and permeability. In light of the changes of ECs elicited by ALDH1A1 in melanoma cells, the present study explored the release of cytokines involved in the angiogenesis process from melanoma cells pre-treated with CM037, a selective ALDH1A1 blocker. CM037 (10 μM) produced a substantial decline of enzymatic activity in both A375 and WM-266-4 cells (Fig. S2A and S2B), while it did not affect cell survival (Fig. S2C and D).

When ALDH1A1 was inhibited, in both melanoma cell lines, an altered secretion of angiogenesis inducers with a drastic reduction of VEGF (-6.18 fold and -8.04 fold in A375 and WM-266-4, respectively) (Fig. 2B and D) and IL-8 release (-8.18 fold and -5.06 fold in A375 and WM-266-4, respectively) was found (Fig. 2A and C). IL-8 has been demonstrated to positively influence the melanoma microenvironment and ECs in an autocrine and paracrine manner (31). By contrast, in CM037-treated A375 a relevant increase of anti-angiogenic factors such as IL-12 and plasminogen activator inhibitor, type I (PAI-1) (+6.41 and +2.56 fold, respectively) was observed (Fig. 2B). Similarly, in CM037 treated WM-266-4 a substantial increase in the anti-angiogenic IL-6 (+67.03 fold) and IL-12 (+2,34 fold) compared with untreated cells was observed (Fig. 2C and D), highlighting the contribution of the ALDH1A1 enzyme activity to melanoma angiogenic phenotype. Based on these results, the present study focused on IL-8. Indeed, overexpression of IL-8 is related to melanoma angiogenesis and metastases (32,33). In melanoma cells expressing different levels of ALDH1A1, it was found that high ALDH1A1 expression was associated with a significant increase of soluble IL-8 levels compared with melanoma ALDH1A1KD (Fig. 2E and F). In agreement with array panel

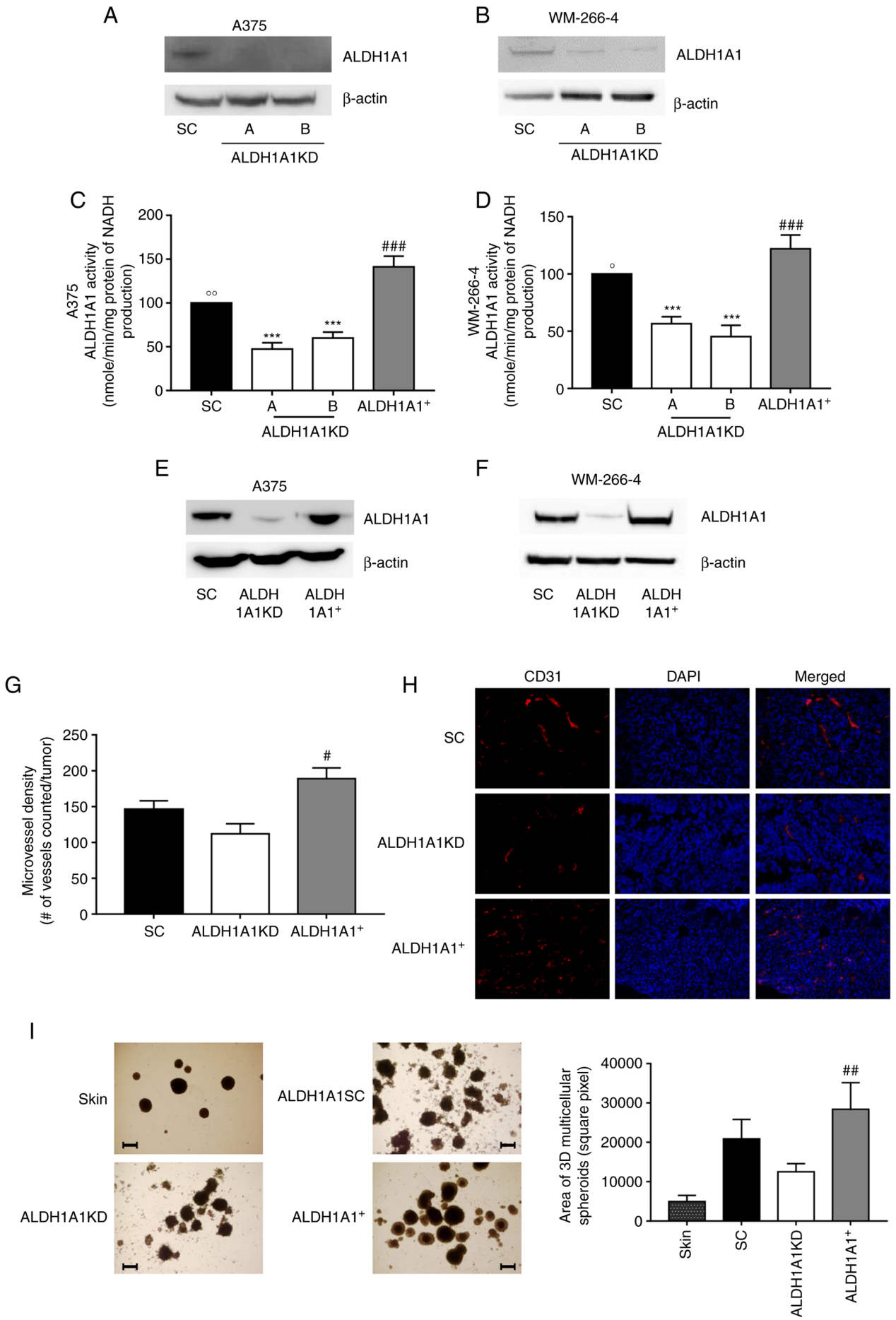

Figure 1. Continued.

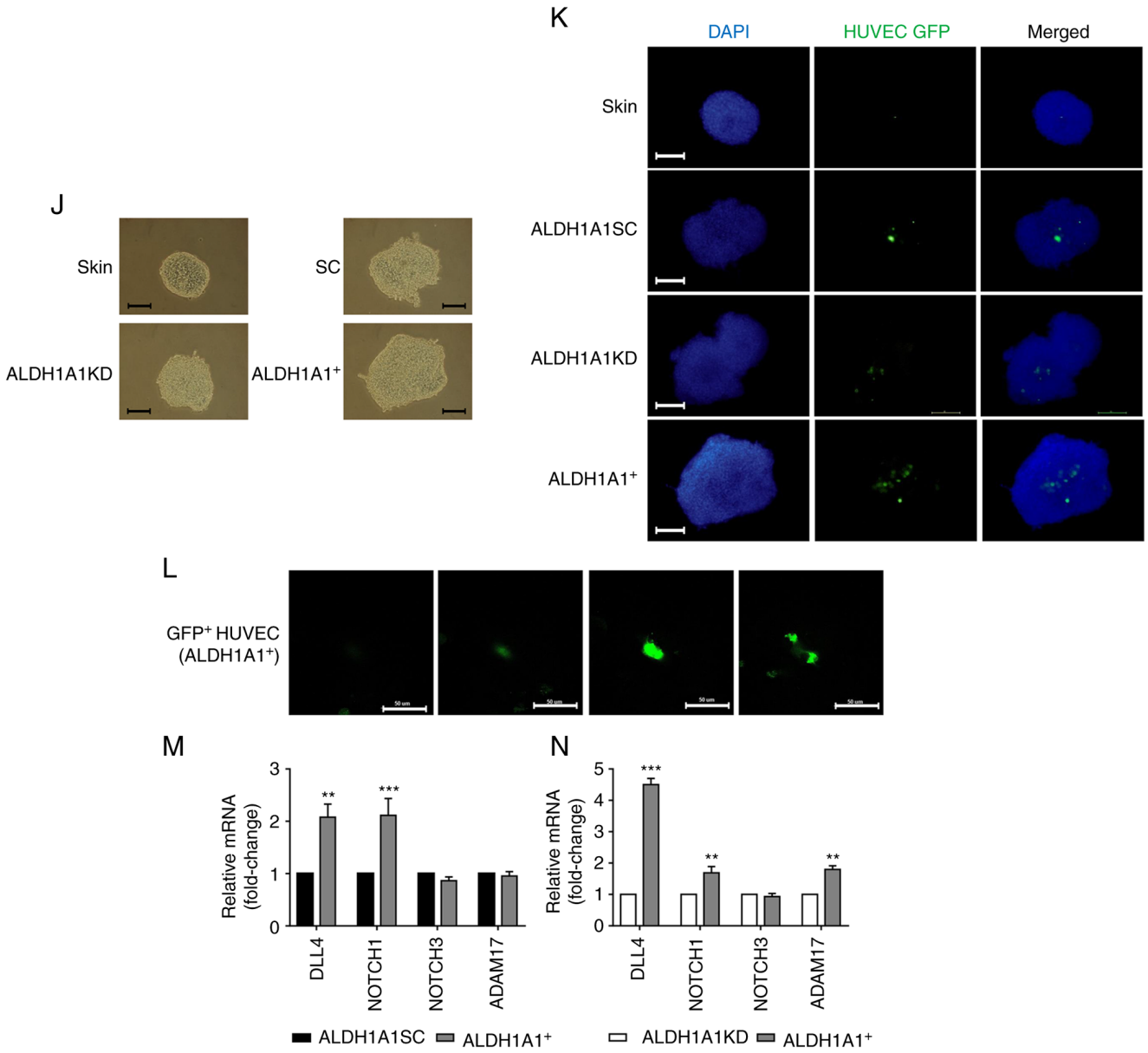

Figure 1. Melanoma ALDH1A1 promoted HUVECs recruitment and modulated endothelial Notch signaling in a model of 3D multicellular melanoma tumorspheres. Loss-of function and gain-of function validation was used to study ALDH1A1 expression in melanoma cells. Western blot analysis of (A) A375 and (B) WM-266-4 (ALDH1A1SC and ALDH1A1KD, clones shA and shB) cultured in 10% FBS for 48 h. Enzymatic activity in (C) A375 and (D) WM-266-4 evaluated by NADH production. ***P<0.001 vs. ALDH1A1SC; $^{\#\#\#}$P<0.001 vs. ALDH1A1KD; °P<0.05 and °°P<0.01 vs. ALDH1A1$^+$. Western blot analysis of (E) A375 and (F) WM-266-4 cultured in 10% FBS for 48 h. β-actin was used as loading control. Blot representative of three experiments. (G) Quantification of microvessel density by CD31 staining was performed counting 5 random fields for section, each slide having five sections (magnification, x2). $^{\#}$P<0.05 vs. ALDH1A1KD group. (H) Representative images of immunostaining for CD31 (red) and DAPI (blue) in tumor sections from ALDH1A1SC (top), ALDH1A1KD (center) or ALDH1A1+ (bottom) mice. Images show different vessel densities in tumors. Magnification, x20. (I) Bright-field image (magnification, x4) of skin 3D spheroids and multicellular melanoma 3D tumorspheres consisting in A375 cells, HaCaT, NHDF and HUVECs co-cultured in ultralow attachment plates for 6 days. Scale bar=100 μm. Quantification of 3D multicellular spheres. The area occupied by spheres was calculated using Fiji Software and three images for each well were quantified. Spheres >100 pixel square were considered. $^{\#\#}$P<0.01 vs. ALDH1A1KD. (J) Bright-field images obtained at magnification x20 after fixation in paraformaldehyde and mounting in Fluoromount aqueous mounting medium. Scale bar=50 μm. (K) GFP-HUVECS localization in skin and melanoma 3D models. Fluorescence imaging demonstrated distribution of ECs (green) inside 3D spheroids. Merged images show blood vessel-like tubules of green HUVECs (x20 magnification). Scale bar=50 μm. (L) Z-stack images obtained through a confocal microscope show bifurcation of HUVECs tubules in A375 ALDH1A1$^+$ 3D tumorspheres (magnification, x63; scale bar=50 μm). (M) Notch pathway genes in HUVECs co-cultured with A375 ALDH1A1$^+$ vs. HUVECs co-cultured with A375 ALDH1A1SC sorted from multicellular melanoma 3D tumorspheres. Data are reported as fold change relative to A375 ALDH1A1SC, assigned to 1. **P<0.01 and ***P<0.001 vs ALDH1A1SC. (N) Notch pathway genes under/overexpressed in HUVECs co-cultured with the A375 ALDH1A1$^+$ cells vs. HUVECs co-cultured with the A375 ALDH1A1KD cells sorted from multicellular melanoma 3D tumorspheres. **P<0.01 and ***P<0.001 vs ALDH1A1KD. Data are reported as fold change relative to A375 ALDH1A1KD, assigned to 1. HUVECs, human umbilical vein endothelial cells; SC, scrambled control; GFP, green fluorescent protein; ECs, endothelial cells.

results, A375 showed greater IL-8 release compared with WM-266-4.

High protein levels were associated with increased IL-8 gene expression in A375 ALDH1A1$^+$ compared with A375 ALDH1A1KD, indicating that ALDH1A1 modulates IL-8 levels at the transcriptional level (Fig. S3A). As the ALDH1 family is required for retinoic acid (RA) biosynthesis, the present study investigated whether RA signaling

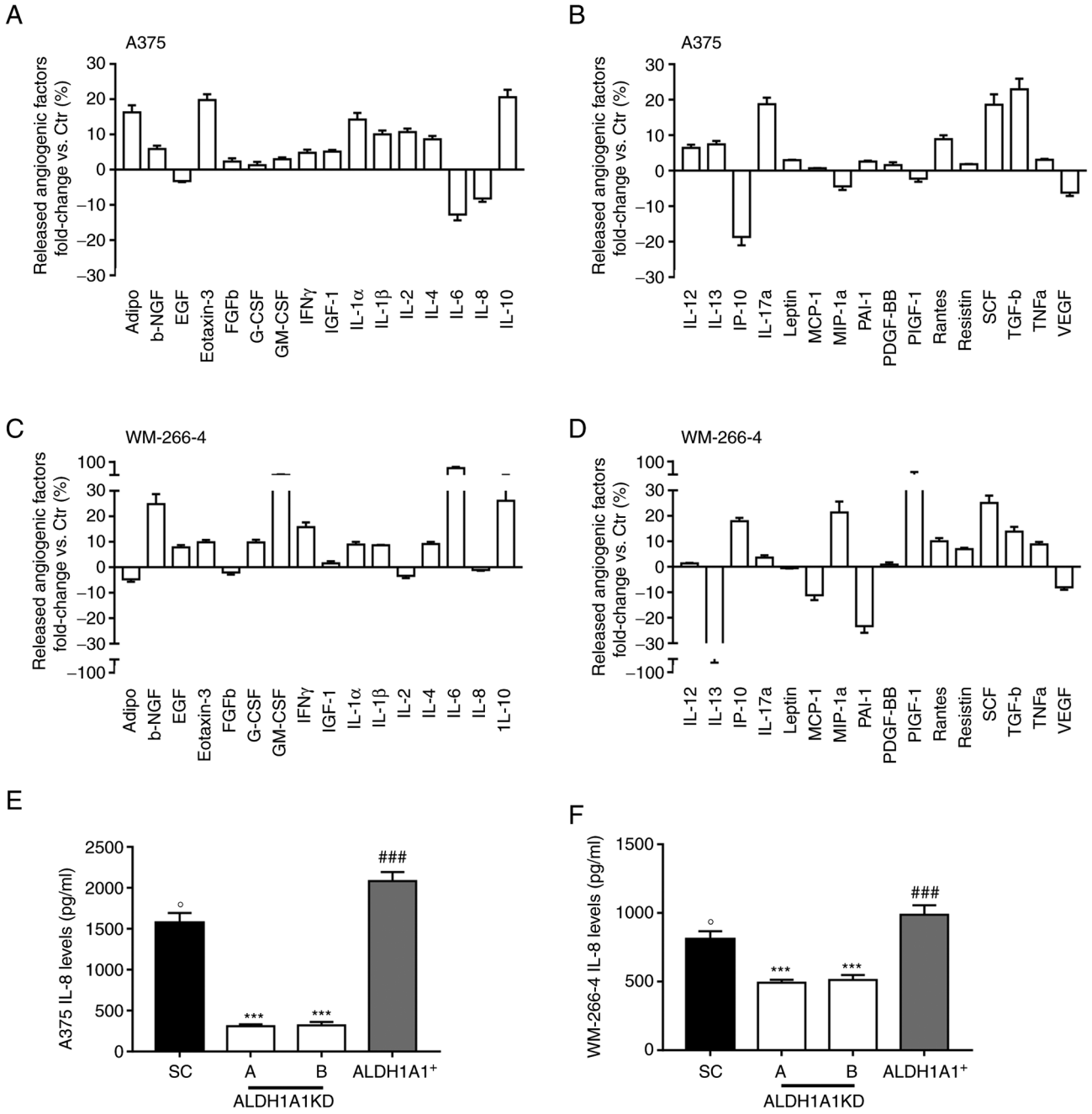

Figure 2. ALDH1A1 in melanoma cells regulates angiogenic factors release. Angiogenic factors release evaluated by ELISA plate array in supernatants of (A and B) A375 and (C and D) WM-266-4 treated or not treated with CM037 (1 μM) for 48 h. The experiment was performed twice in duplicate. Data are reported as percentage of fold change of CM037 treated vs. Ctr. Soluble IL-8 was detected by ELISA in media conditioned by (E) A375 and (F) WM-266-4. Cells were seeded in 24-well plates at density $3x10^4$ cells/well. After 48 h the supernatants were harvested and cells fixed, stained and counted. The number of counted cells was not significantly different. Data are reported as pg/ml. The level of expression for each specific cytokine is directly proportional to the luminescence intensity. ***P<0.001 vs. ALDH1A1SC. $^{###}$P<0.001 vs. ALDH1A1KD. °P<0.05 vs. ALDH1A1$^+$. Ctr, untreated cells.

might mediate the observed ALDH1A1-dependent IL-8 regulation in A375. Exposure of A375 ALDH1A1SC and A375 ALDH1A1$^+$ to RA receptor inhibitor (AGN 193109) reduced IL-8 gene expression (Fig. S3B), while exposure of A375 ALDH1A1KD to exogenous RA increased it (Fig. S3C). Furthermore, in A375 ALDH1A1KD, RA promoted nuclear localization of NF-κB, one of the transcription factors of IL-8 genes (Fig. S3D) and increased NF-κB-p65 subunit expression (Fig. S3E), suggesting the existence of an RA-NF-κB axis in ALDH1A1-mediated IL-8 expression.

Next, whether and how ALDH1A1 expression in melanoma cells influenced endothelium was investigated, specifically focusing on the communication between melanoma and ECs. The present study generated a 2D co-culture model of ECs and melanoma cells cultured in the Transwell system. HUVECs proliferation, scratch assay, tube formation and permeability and cellular features of angiogenesis were assessed.

Fig. 3A and B show a decreased proliferation of HUVECs when co-cultured with A375 ALDH1A1KD and WM-266-4 ALDH1A1KD, respectively, compared with

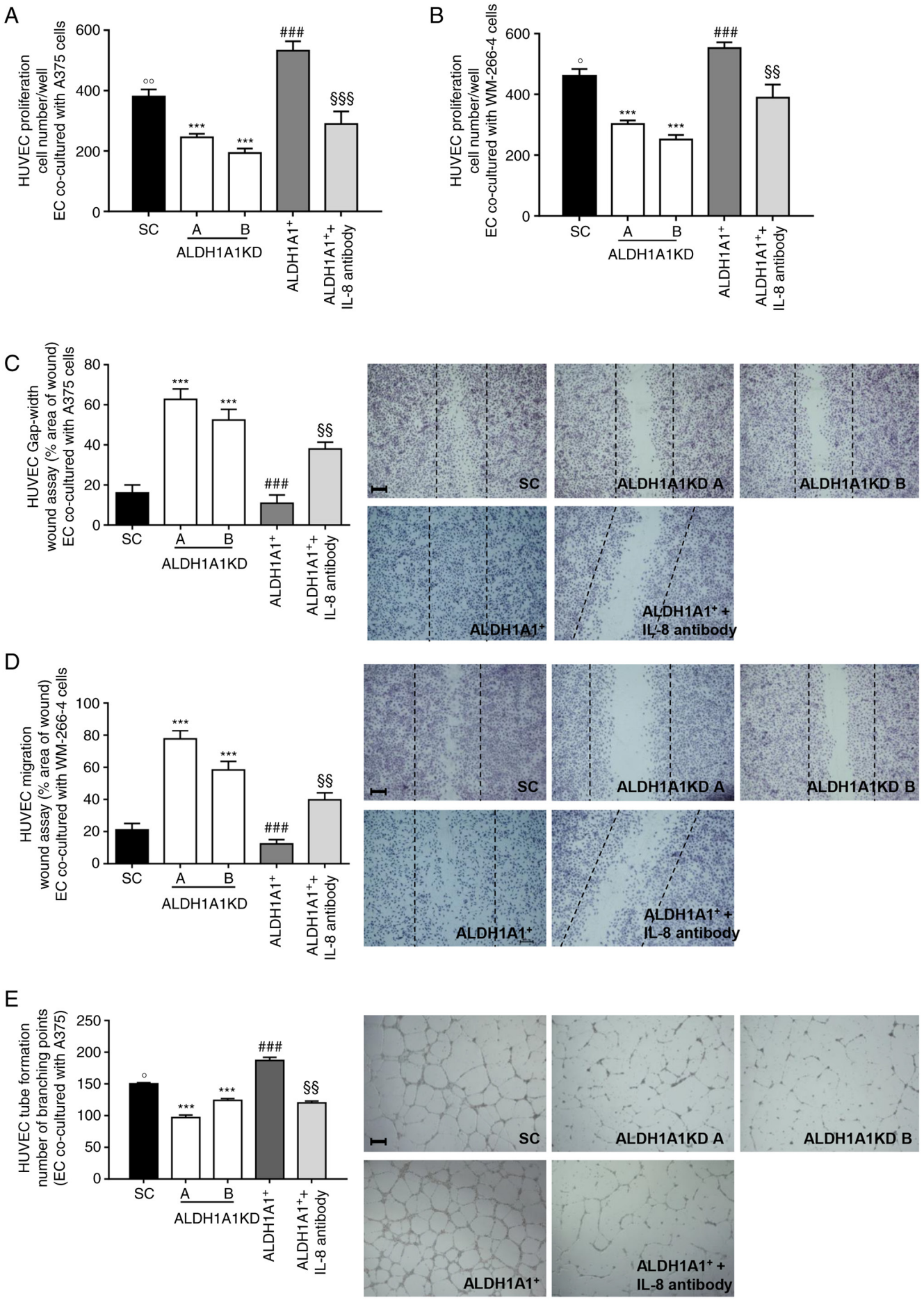

Figure 3. Continued.

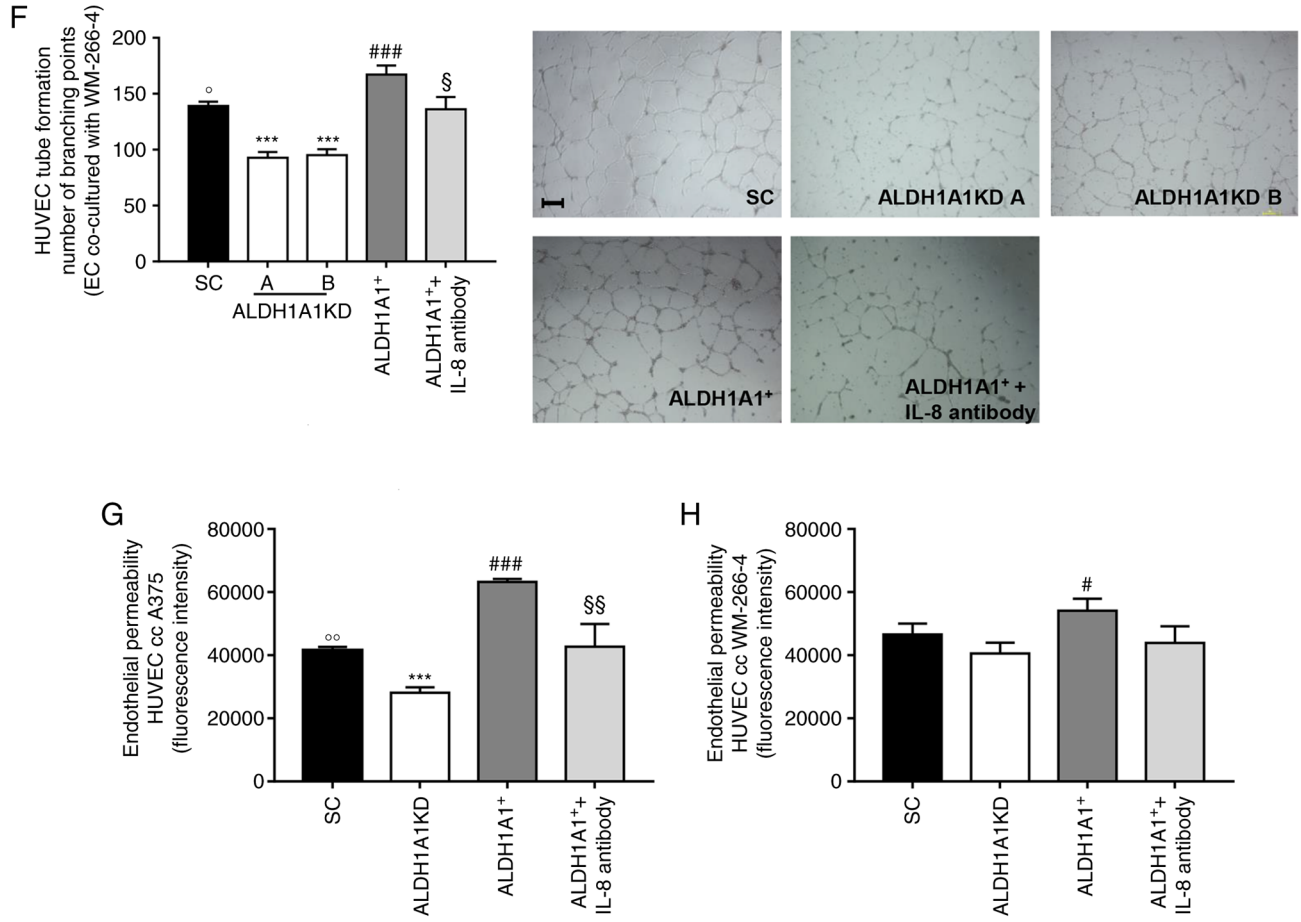

Figure 3. Melanoma ALDH1A1 regulated endothelial angiogenic features in an IL-8 dependent-manner. Proliferation of HUVECs co-cultured with (A) A375 and (B) WM-266-4. Melanoma cells were co-cultured with HUVECs for 48 h (1% FBS); HUVECs were fixed, stained and counted (five fields random for well). Data are reported as number of HUVECs counted/well. (n=3). ***P<0.001 vs. HUVECs co-cultured with melanoma ALDH1A1SC. ###P<0.001 vs. HUVECs co-cultured with melanoma ALDH1A1KD. °P<0.05 and °°P<0.01 vs. HUVECs co-cultured with melanoma ALDH1A1+. §§P<0.01 and §§§P<0.001 vs. melanoma ALDH1A1+. Scratch assay of HUVECs co-cultured with (C) A375 and (D) WM-266-4. Melanoma cells were co-cultured with HUVECs for 18 h (1% FBS). Data are reported as percentage of area of gap width (percentage of area at 18 h/area at 0 h). ***P<0.001 vs. HUVECs co-cultured with melanoma ALDH1A1SC. ###P<0.001 vs. HUVECs co-cultured with melanoma ALDH1A1KD. §§P<0.01 vs. melanoma ALDH1A1+. Representative images of HUVECs monolayer; scale bar=100 μm. (E) Quantification and representative images (magnification, x4) of branching points quantified by using Fiji Software of HUVECs seeded in Matrigel layer and co-cultured A375 for 18 h (1% FBS). The results represent the media of five images. ***P<0.001 vs. HUVECs co-cultured with A375 ALDH1A1SC. ###P<0.001 vs. HUVECs co-cultured with A375 ALDH1A1KD; °P<0.05 vs. HUVECs co-cultured with melanoma ALDH1A1+. §§P<0.01 vs. melanoma ALDH1A1+. Scale bar 100 μm (F) Quantification and representative images of HUVECs network (magnification, x4) of branching points using Fiji Software of HUVECs seeded in Matrigel layer and co-cultured with WM-266-4 for 18 h (1% FBS). The results represent the mean of the quantification from five images. Scale bar=100 μm ***P<0.001 vs. HUVECs co-cultured with WM-266-4 ALDH1A1SC. ###P<0.001 vs. HUVECs co-cultured with WM-266-4 ALDH1A1KD; °P<0.05 vs. HUVECs co-cultured with melanoma ALDH1A1+. §P<0.05 vs. melanoma ALDH1A1+. Permeability of HUVECs co-cultured with melanoma cells (G) A375 and (H) WM-266-4. Tumor cells were seeded at the bottom of 12-well plates with HUVECs in Transwells. The cells have been maintained in co-culture until HUVECs monolayer formation in presence or not of IL-8 neutralizing antibody (80 ng/ml; n=3). ***P<0.01 vs. HUVECs co-cultured with melanoma ALDH1A1SC. #P<0.05 and ###P<0.001 vs. HUVECs co-cultured with melanoma ALDH1A1KD. °°P<0.01 vs. HUVECs co-cultured with melanoma ALDH1A1+. §§P<0.01 vs. melanoma ALDH1A1+. HUVECs, human umbilical vein endothelial cells; SC, scrambled control.

that from ALDH1A1SC cells. Similar results were obtained when ALDH1A1 in melanoma cells was blocked by CM037 (Fig. S4A and B). By contrast, the co-incubation of HUVECs with A375 ALDH1A1+ and WM-266-4 ALDH1A1+ cells enhanced proliferation of ECs (Fig. 3A and B) and IL-8 neutralizing antibody blunted this effect. EC migration was then analyzed by scratch assay and a significant reduction of HUVECs motility when co-cultured with A375 ALDH1A1KD (Fig. 3C) and WM-266-4 ALDH1A1KD cells (Fig. 3D) was found compared with ALDH1A1SC melanoma cells. In the same experiments, melanoma cells ALDH1A1+ provided a pro-migratory stimulus for endothelium (Fig. 3C and D), mitigated by IL-8 neutralizing antibody addition. In addition, the ability of melanoma cells to induce HUVECs motility was abolished when CM037 inhibited ALDH1A1 (Fig. S4C for A375 and S4D for WM-266-4 cells).

Tube formation assay results further corroborated these effects. When co-cultured with A375 ALDH1A1+ (Fig. 3E) and WM-266-4 ALDH1A1+ (Fig. 3F), HUVECs showed a strong ability to form net-like structures, which was significantly reduced when co-cultured in the presence of IL-8 neutralizing antibody. A marked reduction in tube formation was also observed when HUVECs were incubated with A375 ALDH1A1KD and WM-266-4 ALDH1A1KD cells (Fig. 3E and F). Similarly, pharmacological inhibition of ALDH1A1 resulted in an impairment of angiogenic sprouting

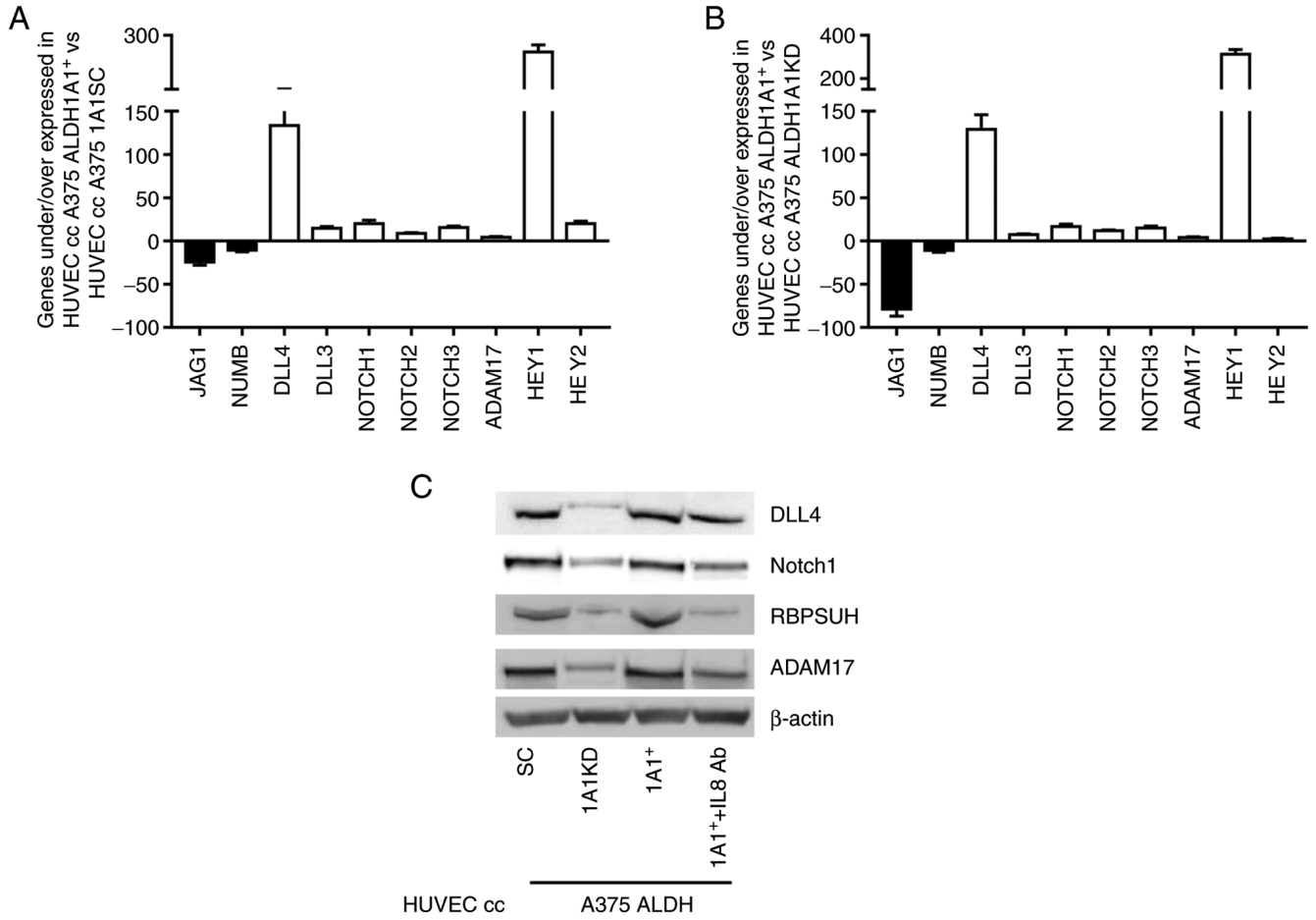

Figure 4. Melanoma ALDH1A1 affects Notch signaling in HUVECs in 2D co-culture (Transwell system). (A) Notch pathway genes under/over expressed in HUVECs co-cultured with A375 ALDH1A1$^+$ vs. HUVECs co-cultured with A375 ALDH1A1SC. (B) Notch pathway genes under/over expressed in HUVECs co-cultured with A375 ALDH1A1$^+$ vs. HUVECs co-cultured with A375 ALDH1A1KD. Co-cultures were maintained for 6 days The experiment was performed twice in duplicate. (C). Evaluation of Notch signaling mediators DLL4, Notch1, RBPSUH and ADAM17 in HUVECs alone or co-cultured with A375 clones for 6 days. β-actin was used as loading control. The experiment was repeated three times. HUVECs, human umbilical vein endothelial cells; HUVECcc, HUVECs co-cultured; DLL4, delta-like canonical Notch ligand 4; RBPSUH, recombining binding protein, suppressor of hairless; ADAM17, A disintegrin and metalloproteinase-17.

of HUVECs co-cultured with both melanoma cell lines (A375, Fig. S4E and WM-266-4 S4F).

Similar results were obtained by measuring endothelial permeability. HUVECs co-cultured with melanoma ALDH1A1$^+$ cells were more permeable compared with HUVECs co-cultured with ALDH1A1KD cells counterpart (Fig. 3G for A375 and Fig. 3H for WM-266-4). A neutralizing antibody to IL-8 significantly inhibited the permeability of HUVECs (Fig. 3G and H).

Collectively, these findings demonstrated the existence of dynamic crosstalk between melanoma and ECs which acquired an angiogenic phenotype, promoted by tumor ALDH1A1 expression and activity through, at least in part, the release of NF-κB associated IL-8. Of note, in HUVECs, at concentration similar to that measured in the medium of melanoma cells, exogenous IL-8 was able to promote cell proliferation (Fig. S4G).

Tumor ALDH1A1 effects Notch signaling in ECs through IL-8. To investigate the underlying mechanisms by which tumor ALDH1A1 affects the endothelial angiogenic program, a Notch signaling gene array was performed on ECs co-cultured with melanoma cells using the Transwell system. A long-term 2D co-culture (6 days) was performed with HUVECs and A375 cells to mimic the co-existence of melanoma and ECs in 3D tumorspheres. Profiling the expression of 84 genes involved in Notch signaling, an impressive gene rearrangement between endothelium grown alone and co-cultured with melanoma cells was found (Fig. S5). The present study focused on Notch ligands, receptors and downstream effectors involved in angiogenesis. Delta-like ligand 4 (DLL-4) is the most important Notch ligand for early vascular development and angiogenesis (34). DLL-4 gene expression was strongly induced in HUVECs incubated with A375 ALDH1A1$^+$ compared with HUVECs co-cultured with A375 ALDH1A1SC and A375 ALDH1A1KD (>133 and 128 fold, respectively) (Fig. 4A and B). An important increase of DLL-3 was observed in ECs derived from 2D co-cultures with melanoma ALDH1A1$^+$ compared with other settings. By contrast, another Notch ligand gene, Jagged1 (Jag1), which can compete with DLL4 to negatively regulate angiogenesis (34), was markedly downregulated in HUVECs co-cultured with A375ALDH1A1$^+$ when compared with A375 ALDH1A1SC (-24.29 fold) and A375 ALDH1A1KD (-78.76 fold; Fig. 4A and B).

As with the ligands, the Notch receptors also serve important roles in angiogenesis (35). Expression of all three Notch1, Notch2 and Notch3 genes was upregulated in HUVECs co-cultured with A375 ALDH1A1$^+$ when compared with HUVECs co-cultured with A375 ALDH1A1SC and A375 ALDH1A1KD. Notch1 is the most important receptor of the Notch signaling cascade involved in early angiogenesis. A +19.98 and +16.71 fold increase in HUVECs co-cultured with A375 ALDH1A1$^+$ was observed compared with HUVECs co-cultured with A375 ALDH1A1SC and A375 ALDH1A1KD, respectively. Similar regulation was observed for the Notch2 gene (+14.92 fold in HUVECs co-cultured with A375 ALDH1A1$^+$ vs. A375 ALDH1A1KD, +15.45 fold vs. A375 ALDH1A1SC) and Notch3 gene (+11.89 fold in HUVECs co-cultured with A375 ALDH1A1$^+$ vs. A375 ALDH1A1KD and +8.87 fold vs. ALDH1A1SC) (Fig. 4A and B).

The binding of Notch receptors with ligands promotes the proteolytic cleavage of the Notch receptors, mediated by ADAM-family metalloproteases (36). The array showed an upregulation in gene expression of ADAM17, one of the main proteases involved in Notch signaling, in endothelium co-cultured with A375 ALDH1A1$^+$ when compared with A375 ALDH1A1SC (+4.26 fold) and A375 ALDH1A1KD (+4.10 fold; Fig. 4A and B).

The canonical Notch target genes, such as the HEY family, were also significantly affected by tumor ALDH1A1 levels. HEY1 showed an increase of expression by 253 fold in HUVECs co-cultured with A375 ALDH1A$^+$ compared with HUVECs co-cultured with A375 ALDH1A1SC and reached >300 fold when compared with HUVECs incubated with A375 ALDH1A1KD (Fig. 4A and B). HEY2 gene showed a lower variation within different experimental settings. This gene was overexpressed ~2.3 fold in HUVECs co-cultured with A375 ALDH1A1$^+$ vs. HUVECs incubated with A375 ALDH1A1KD (Fig. 4A and B). An increase of ~20.01 fold was observed in HUVECs co-cultured with A375 ALDH1A1SC vs. HUVECs grown with A375 ALDH1A1$^+$ (Fig. 4A and B).

By contrast, the present study found a decrease of NUMB gene, an inhibitory Notch pathway regulator, in HUVECs co-cultured with A375 ALDH1A1$^+$ compared with both A375 ALDH1A1SC (- 10.59 fold) and A375 ALDH1A1KD (-10.87 fold; Fig. 4A and B).

Evidence supports the idea that pro-inflammatory stimuli can activate Notch signaling in different cellular contexts (37). Thus, the present study explored the involvement of IL-8 in the modulation of protein expression of Notch pathway driven by melanoma ALDH1A1 in the 2D co-culture model of ECs and A375 cells in the presence of IL-8-neutralising antibody. Western blot analysis in ECs corroborated the gene array results (Fig. 4C). An increase of DLL4 protein expression in ECs co-cultured with A375 ALDH1A1$^+$ was found compared with endothelium incubated with A375ALDH1A1KD and treatment of co-cultures with IL-8-neutralising antibody significantly reduced DLL4 expression. Furthermore, Notch1 and ADAM17 expression in ECs was also influenced by melanoma ALDH1A1 levels and IL-8 treatment, indicating that IL-8 released by melanoma cells contributes to Notch signaling modification (Fig. 4C). Finally, the present study analyzed the RBPSUH expression. When Notch signaling is activated, BPSUH promotes genes transcription leading to activation of Notch target genes (38). The present study found a high RBPSUH expression in HUVECs co-cultured with A375 ALDH1A1$^+$ compared with HUVECs co-cultured with A375 ALDH1A1KD and IL-8 neutralizing antibody blunted this effect.

Altogether, these data linked tumor ALDH1A1 levels and secreted IL-8 to Notch signaling activation in the endothelium.

Discussion

The present study aimed to assess the contribution of melanoma ALDH1A1 on tumor angiogenesis and to characterize the molecular signature of endothelium co-cultured with melanoma cells in 2D and 3D *in vitro* settings. The results showed dynamic crosstalk between tumor melanoma cells and endothelium, partly mediated by IL-8 release from melanoma cells and favored by tumor ALDH1A1 overexpression and activity. In particular, IL-8 induced the expression in normal ECs of key mediators involved in the activation of Notch signaling associated with the angiogenic phenotype.

Increased metabolism of toxic aldehydes through ALDH upregulation promotes cancer progression and therapy resistance. ALDH1A1 is a cytosolic enzyme expressed in several solid tumors (39), where it confers stem-like phenotype and aggressive features. We and other research groups have demonstrated that the acquisition of stem-like phenotype driven by ALDH1A1 in breast cancer cells is implicated in tumor vascularization (40,41) and angiogenesis through tumor HIF-1α/VEGF signaling pathway activation and VEGF paracrine action on ECs (17). A role of ALDH1A1 in melanoma pathogenesis has also been suggested in recent studies (42,43), but no direct evidence for a functional role in melanoma angiogenesis has been reported. In the present study, *in vivo* experiments demonstrated a role of ALDH1A1 overexpression with increased microvessel density in tumor xenografts. Moreover, by using a 2D ECs-melanoma model and a 3D model of multicellular tumorspheres, the present study found a differential endothelial angiogenic phenotype mediated by tumor ALDH1A1 expression levels and IL-8 release. Multicellular melanoma tumorspheres were generated to recapitulate the global tumor tissue organization and create a more complex TME than 2D culture (20,44). Normal ECs and fibroblasts were included in the 3D constructs to assess the role of variable ALDH1A1 expression in tumor cells in conditioning the other cells, focusing on the endothelium. Increased infiltration and organization of HUVECs were found in the core of A375 ALDH1A1$^+$ tumorspheres, presumably linked with activation of HIF-1α signaling mediated by ALDH1A1 (17). Indeed, HIF-1α is a master transcriptional factor for angiogenesis and metabolic remodulation of tumor cells (45).

The crosstalk between tumor cells and their microenvironment is crucial for cancer cell self-renewal, tumor growth and metastasis (46). Nevertheless, the metabolic modulation of the endothelium and the formation of a deregulated and aberrant tumor vasculature serve a critical role in maintaining the stem-like status in tumors (47). Notably, Notch pathway activation by signals within the TME has been proposed as an additional mechanism by which endothelium controls the activity of stem-like cells, which in turn influence the pro-angiogenic status of ECs in a vicious cycle (48).

In the 3D co-culture model of the present study, HUVECs from multicellular A375 ALDH1A1$^+$ tumorspheres expressed higher levels of *Notch1* and *DLL4* genes when compared with A375 ALDH1A1KD. DLL4-Notch signaling has been implicated in the specification of the endothelial tip cells (48) and tumor vasculature has been shown to overexpress DLL4, as endothelial-specific loss of DLL-4 resulted in tumor vessel regression along with a reduction in both epithelial-mesenchymal transition and stem-like features in tumor cells (49).

In agreement with the evidence gathered in tumorspheres, high ALDH1A1 expression in A375 and WM-266-4 cells promoted HUVECs proliferation, migration, tube formation and hyperpermeability in a 2D co-culture model. Conversely, loss of function experiments produced a marked decrease of endothelial pro-angiogenic functions when co-cultured with melanoma cells silenced for ALDH1A1. Moreover, exposure of melanoma cells to the enzyme inhibitor CM037, significantly impaired the angiogenic features of the endothelium, suggesting that both expression and activity of melanoma ALDH1A1 are critical for the acquisition of ECs of an angiogenic phenotype.

The present study identified IL-8 as one of the downstream target of ALDH1A1, responsible for endothelium phenotype remodeling. IL-8 is constitutively expressed in melanoma (50); however, it is unknown which factors mediate its upregulation in tumors. A hypothetical mechanism might involve tumor hypoxia. *In vivo* studies in human melanoma and other tumors show an increase in IL-8 production mediated by hypoxia and acidosis of the microenvironment (51,52). Another mechanism may involve the signaling of RA (53,54), one of the main products of ALDH1A1 activity (39). Although the RA receptor (RAR) may regulate the transcription of cytokines genes, the promoter regions of a number of cytokines do not contain any RA responsive elements, supposing an indirect role of RAR in genes regulation (55) through the activation of transcription factors. The binding of NF-κB to the IL-8 promoter is required for triggering IL-8 gene transcription, with p65 as the subunit responsible for binding to the promoter (56-59). Furthermore, in a model of melanoma cell line, RA in combination with TNFα, is able to induce IL-8 expression with the contribution of NF-κB (60,61). The present study showed that exogenous RA promoted IL-8 expression in A375 ALDH1A1SC, as well NF-κB nuclear translocation and NF-κB-p65 subunit expression, while RAR inhibition in A375 ALDH1A1SC and ALDH1A1$^+$ decreased IL-8 expression, suggesting that ALDH1A1 mediated IL-8 expression and production by RA-NF-κB signaling pathway. However, whether alternative and/or complementary pathways are involved, requires further investigations. A critical function for this chemokine in establishing stem-like properties of a number of solid tumors has been reported (62) and involvement of IL-8 in tumor progression has also been demonstrated (63).

IL-8 influences tumor growth, angiogenesis, invasion and metastasis through autocrine and paracrine signaling (32,33,64) by binding two cell-surface G protein-coupled receptors (CXCR1 and CXCR2) (65). Cytokines, including IL-8, can induce Notch signaling (66), but the mechanism remains unclear. Notch signaling serves a critical role in the overall regulation of tumor angiogenesis (67). The present study found a differential Notch pathway gene and protein expression profile in ECs co-cultured with melanoma cells, depending on melanoma ALDH1A1 expression and activity and IL-8 release and paracrine activity on ECs. By comparing the expression of Notch mediators in ECs derived from different multicellular 3D tumorspheres, it was found that high ALDH1A1 expression in melanoma cells was associated with higher expression of ligands *DLL3* and *DLL4*. DLL4 is a critical Notch ligand for stimulating angiogenesis (68). Contrarily, the gene expression of another Notch ligand, *Jag1*, which can compete with DLL4 to negatively regulate angiogenesis (69), was drastically reduced. In the models of the present study, the Notch receptors and downstream effectors were influenced by melanoma ALDH1A1. The expression of Notch1, Notch2 and Notch3 receptors and ADAM17 (which cleaves the receptors), as well as the Notch target genes HEY1 and HEY2, were induced in ECs grown with melanoma ALDH1A1$^+$. Consistently, a reduction of NUMB gene expression, an inhibitory Notch pathway regulator, was observed. When protein analysis of the Notch pathway was performed in ECs co-cultured in the presence of IL-8 neutralizing antibody, a reduction of DLL4, Notch1 and ADAM17 protein expression was observed. These findings suggested that ALDH1A1 possibly through IL-8 release, remodels TME, controlling ECs pro-angiogenic phenotype through Notch signaling regulation. The mechanism by which IL-8 activates the Notch pathway remains to be elucidated. Data suggest that IL-8 may interact with VEGF receptor 2 (VEGFR2, the receptor primarily involved in Notch signaling activation), promoting angiogenesis through receptor transactivation (70,71). However, whether IL-8 promotes activation of the Notch pathway in ECs through transactivation of VEGFR2 or direct activation of CXCR1 and CXCR2 remains to be elucidated. Nevertheless, that the modulation of the gene and protein expression profile of Notch pathway mediators in the endothelium in 3D tumorspheres may be partly attributed to direct cell-cell and cell-matrix activity mediated by melanoma cells expressing different levels of ALDH1A1 cannot be excluded.

Together, the present study provided further insight into the mechanisms underlying angiogenesis and tumor progression driven by ALDH1A1 in melanoma cancer cells and described the concerted flow of signals from tumor to ECs. Considering the functional changes in endothelium caused by ALDH1A1 overexpression in melanoma cell lines, this enzyme may cause an extensive remodeling on TME to sustain tumor progression and maintain stem-like phenotype.

In conclusion, ALDH1A1 is a cytosolic enzyme upregulated in tumor cells and involved in detoxifying cells from reactive aldehydes, such as retinaldehyde. This enzyme also engages in acquired resistance to chemotherapeutic drugs, such as oxazolidine, taxanes and platinum derivatives. It is a marker of stemness in several solid tumors and correlates with poor clinical outcome in a number of cancers (72,73). The present study showed that there is also a relationship between ALDH1A1 expression and activity and tumor angiogenesis, through the upregulation of several pro-angiogenic mediators, including the chemokine IL-8. RA-derived ALDH1A1 appeared to be involved in IL-8 expression through NF-κB activation and expression. In TME, tumor-derived IL-8 activated Notch signaling on ECs and promotes the acquisition of a pro-angiogenic phenotype. Based on the role of ALDH1A1 in the control of TME by melanoma,

the enzyme is a promising marker of cross-talk between tumor (stem) cells and ECs, which in turn could be an interesting target for development of new treatments.

Acknowledgements

The authors would like to thank Professor Ambra Grolla, Department of Drug Science, University of Piemonte Orientale A. Avogadro, Novara (Italy) who generously provided cells. The authors would also like to thank Professor Donata Medaglini and Dr Annalisa Ciabattini, Department of Medical Biotechnology, University of Siena, Siena (Italy) for their technical support.

Funding

This work was funded by Regione Toscana-Bando Ricerca Salute 2018_CORELAB and Fondazione Umberto Veronesi, Milan, Italy (Post-doctoral Fellowship 2022).

Availability of data and materials

The datasets used and/or analyzed in the current study are available from the corresponding author upon reasonable request.

Authors' contributions

SD, MZ and VC conceived the present study. VC, ET, AF and ER performed methodology, validation, investigation, data analysis. VC wrote the original draft of the manuscript. SD, LM and MZ wrote reviewed and edited the manuscript. SD supervised and administered the project and acquired funding. All authors reviewed and approved the final manuscript.

Ethics approval and consent to participate

The animal study was conducted according to the guidelines of the Declaration of Helsinki and the Italian law (Legislative Decree no. 26, 4 March 2014), which acknowledges the European Directive 2010/63/UE and was approved by the animal welfare board of University of Siena and the Italian Ministry of Health (authorization no. 62/2014-B).

Patient consent for publication

Not applicable.

Competing interests

The authors declare that they have no competing interests.

References

1. Tripp MK, Watson M, Balk SJ, Swetter SM and Gershenwald JE: State of the science on prevention and screening to reduce melanoma incidence and mortality: The time is now. CA Cancer J Clin 66: 460-480, 2016.
2. Rambow F, Marine JC and Goding CR: Melanoma plasticity and phenotypic diversity: Therapeutic barriers and opportunities. Genes Dev 33: 1295-1318, 2019.
3. Klemen ND, Wang M, Feingold PL, Cooper K, Pavri SN, Han D, Detterbeck FC, Boffa DJ, Khan SA, Olino K, *et al*: Patterns of failure after immunotherapy with checkpoint inhibitors predict durable progression-free survival after local therapy for metastatic melanoma. J Immunother Cancer 7: 196, 2019.
4. Li F and Simon MC: Cancer cells don't live alone: Metabolic communication within tumor microenvironments. Dev Cell 54: 183-195, 2020.
5. Hass R, von der Ohe J and Ungefroren H: Impact of the tumor microenvironment on tumor heterogeneity and consequences for cancer cell plasticity and stemness. Cancers (Basel) 12: 3716, 2020.
6. Qin S, Jiang J, Lu Y, Nice EC, Huang C, Zhang J and He W: Emerging role of tumor cell plasticity in modifying therapeutic response. Signal Transduct Target Ther 5: 1-36, 2020.
7. Maishi N and Hida K: Tumor endothelial cells accelerate tumor metastasis. Cancer Sci 108: 1921-1926, 2017.
8. Howard JD, Moriarty WF, Park J, Riedy K, Panova IP, Chung CH, Suh KY, Levchenko A and Alani RM: Notch signaling mediates melanoma-endothelial cell communication and melanoma cell migration. Pigment Cell Melanoma Res 26: 697-707, 2013.
9. Long X, Ye Y, Zhang L, Liu P, Yu W, Wei F, Ren X and Yu J: IL-8, a novel messenger to cross-link inflammation and tumor emt via autocrine and paracrine pathways (Review). Int J Oncol 48: 5-12, 2016.
10. Weinberg F, Ramnath N and Nagrath D: Reactive oxygen species in the tumor microenvironment: An overview. Cancers (Basel) 11: 1191, 2019.
11. Tasdogan A, Faubert B, Ramesh V, Ubellacker JM, Shen B, Solmonson A, Murphy MM, Gu Z, Gu W, Martin M, *et al*: Metabolic heterogeneity confers differences in melanoma metastatic potential. Nature 577: 115-120, 2020.
12. Barrera G: Oxidative stress and lipid peroxidation products in cancer progression and therapy. ISRN Oncol 2012: 137289, 2012.
13. Luo Y, Dallaglio K, Chen Y, Robinson WA, Robinson SE, McCarter MD, Wang J, Gonzalez R, Thompson DC, Norris DA, *et al*: ALDH1A isozymes are markers of human melanoma stem cells and potential therapeutic targets. Stem Cells 30: 2100-2113, 2012.
14. Ma I and Allan AL: The role of human aldehyde dehydrogenase in normal and cancer stem cells. Stem Cell Rev Rep 7: 292-306, 2011.
15. Moreb JS, Baker HV, Chang LJ, Amaya M, Lopez MC, Ostmark B and Chou W: ALDH isozymes downregulation affects cell growth, cell motility and gene expression in lung cancer cells. Mol Cancer 7: 87, 2008.
16. Charafe-Jauffret E, Ginestier C, Iovino F, Tarpin C, Diebel M, Esterni B, Houvenaeghel G, Extra JM, Bertucci F, Jacquemier J, *et al*: Aldehyde dehydrogenase 1-positive cancer stem cells mediate metastasis and poor clinical outcome in inflammatory breast cancer. Clin Cancer Res 16: 45-55, 2010.
17. Ciccone V, Terzuoli E, Donnini S, Giachetti A, Morbidelli L and Ziche M: Correction to: Stemness marker ALDH1A1 promotes tumor angiogenesis via retinoic acid/HIF-1α/VEGF signalling in MCF-7 breast cancer cells. J Exp Clin Cancer Res 37: 311, 2018.
18. Terzuoli E, Bellan C, Aversa S, Ciccone V, Morbidelli L, Giachetti A, Donnini S and Ziche M: ALDH3A1 overexpression in melanoma and lung tumors drives cancer stem cell expansion, impairing immune surveillance through enhanced PD-L1 output. Cancers (Basel) 11: 1963, 2019.
19. Ramamoorthy P, Thomas SM, Kaushik G, Subramaniam D, Chastain KM, Dhar A, Tawfik O, Kasi A, Sun W, Ramalingam S, *et al*: Metastatic tumor-in-a-dish, a novel multicellular organoid to study lung colonization and predict therapeutic response. Cancer Res 79: 1681-1695, 2019.
20. Han SJ, Kwon S and Kim KS: Challenges of applying multicellular tumor spheroids in preclinical phase. Cancer Cell Int 21: 152, 2021.
21. Cerebral Organoid Cryopreservation and Immunofluorescence. https://www.stemcell.com/cerebral-organoid-cryosectioning-immunofluorescence.html
22. Livak KJ and Schmittgen T: D. Analysis of relative gene expression data using real-time quantitative PCR and the 2(-Delta Delta C(T)) method. Methods 25: 402-408, 2001.
23. Ciccone V, Zazzetta M and Morbidelli L: Comparison of the effect of two hyaluronic acid preparations on fibroblast and endothelial cell functions related to angiogenesis. Cells 8: 1479, 2019.

24. Ciccone V, Monti M, Monzani E, Casella L and Morbidelli L: The metal-nonoate Ni(SalPipNONO) inhibits in vitro tumor growth, invasiveness and angiogenesis. Oncotarget 9: 13353-13365, 2018.
25. Flori L, Macaluso M, Taglieri I, Sanmartin C, Sgherri C, Leo MD, Ciccone V, Donnini S, Venturi F, Pistelli L, *et al*: Development of fortified citrus olive oils: From their production to their nutraceutical properties on the cardiovascular system. Nutrients 12: 1557, 2020.
26. Ciccone V, Monti M, Antonini G, Mattoli L, Burico M, Marini F, Maidecchi A and Morbidelli L: Efficacy of AdipoDren® in reducing interleukin-1-induced lymphatic endothelial hyperpermeability. J Vasc Res 53: 255-268, 2016.
27. Samson JM, Menon DR, Smith DE, Baird E, Kitano T, Gao D, Tan AC and Fujita M: Clinical implications of ALDH1A1 and ALDH1A3 mRNA expression in melanoma subtypes. Chem Biol Interact 314: 108822, 2019.
28. Gridley T: Notch signaling in vascular development and physiology. Development 134: 2709-2718, 2007.
29. Rostama B, Peterson SM, Vary CPH and Liaw L: Notch signal integration in the vasculature during remodeling. Vascul Pharmacol 63: 97-104, 2014.
30. Welti J, Loges S, Dimmeler S and Carmeliet P: Recent molecular discoveries in angiogenesis and antiangiogenic therapies in cancer. J Clin Invest 123: 3190-3200, 2013.
31. Srivastava SK, Bhardwaj A, Arora S, Tyagi N, Singh AP, Carter JE, Scammell JG, Fodstad Ø and Singh S: Interleukin-8 is a key mediator of FKBP51-induced melanoma growth, angiogenesis and metastasis. Br J Cancer 112: 1772-1781, 2015.
32. Li A, Dubey S, Varney ML, Dave BJ and Singh RK: IL-8 directly enhanced endothelial cell survival, proliferation, and matrix metalloproteinases production and regulated angiogenesis. J Immunol 170: 3369-3376, 2003.
33. Wu S, Singh S, Varney ML, Kindle S and Singh RK: Modulation of CXCL-8 expression in human melanoma cells regulates tumor growth, angiogenesis, invasion, and metastasis. Cancer Med 1: 306-317, 2012.
34. Fernández-Chacón M, García-González I, Mühleder S and Benedito R: Role of notch in endothelial biology. Angiogenesis 24: 237-250, 2021.
35. Taslimi S and Das S: Angiogenesis and angiogenesis inhibitors in brain tumors. In: Handbook of Brain Tumor Chemotherapy, Molecular Therapeutics, and Immunotherapy. Newton HB (ed) 2nd edition. Academic Press, Cambridge, MA, pp361-371, 2018.
36. Groot AJ and Vooijs MA: The role of adams in notch signaling. Adv Exp Med Biol 727: 15-36, 2012.
37. Fazio C and Ricciardiello L: Inflammation and notch signaling: A crosstalk with opposite effects on tumorigenesis. Cell Death Dis 7: e2515, 2016.
38. Christopoulos PF, Gjølberg TT, Krüger S, Haraldsen G, Andersen JT and Sundlisæter E: Targeting the notch signaling pathway in chronic inflammatory diseases. Front Immunol 12: 668207, 2021.
39. Tomita H, Tanaka K, Tanaka T and Hara A: Aldehyde dehydrogenase 1A1 in stem cells and cancer. Oncotarget 7: 11018-11032, 2016.
40. Ribatti D: Cancer stem cells and tumor angiogenesis. Cancer Lett 321: 13-17, 2012
41. Fan YL, Zheng M, Tang YL and Liang XH: A new perspective of vasculogenic mimicry: EMT and cancer stem cells (Review). Oncol Lett 6: 1174-1180, 2013.
42. Dinavahi SS, Gowda R, Gowda K, Bazewicz CG, Chirasani VR, Battu MB, Berg A, Dokholyan NV, Amin S and Robertson GP: Development of a novel multi-isoform ALDH inhibitor effective as an antimelanoma agent. Mol Cancer Ther 19: 447-459, 2020.
43. Yue L, Huang ZM, Fong S, Leong S, Jakowatz JG, Charruyer-Reinwald A, Wei M and Ghadially R: Targeting ALDH1 to decrease tumorigenicity, growth and metastasis of human melanoma. Melanoma Res 25: 138-148, 2015.
44. Brassard-Jollive N, Monnot C, Muller L and Germain S: In vitro 3D systems to model tumor angiogenesis and interactions with stromal cells. Front Cell Dev Biol 8: 594903, 2020.
45. LaGory EL and Giaccia AJ: The ever-expanding role of HIF in tumour and stromal biology. Nat Cell Biol 18: 356-365, 2016.
46. Whiteside TL: The tumor microenvironment and its role in promoting tumor growth. Oncogene 27: 5904-5912, 2008.
47. Ingangi V, Minopoli M, Ragone C, Motti ML and Carriero MV: Role of microenvironment on the fate of disseminating cancer stem cells. Front Oncol 9: 82, 2019.
48. Jakobsson L, Franco CA, Bentley K, Collins RT, Ponsioen B, Aspalter IM, Rosewell I, Busse M, Thurston G, Medvinsky A, *et al*: Endothelial cells dynamically compete for the tip cell position during angiogenic sprouting. Nat Cell Biol 12: 943-953, 2010.
49. Patel NS, Li JL, Generali D, Poulsom R, Cranston DW and Harris AL: Up-regulation of delta-like 4 ligand in human tumor vasculature and the role of basal expression in endothelial cell function. Cancer Res 65: 8690-8697, 2005.
50. Peng HH, Liang S, Henderson AJ and Dong C: Regulation of interleukin-8 expression in melanoma-stimulated neutrophil inflammatory response. Exp Cell Res 313: 551-559, 2007.
51. Rofstad EK and Halsør EF: Hypoxia-associated spontaneous pulmonary metastasis in human melanoma xenografts: Involvement of microvascular hot spots induced in hypoxic foci by interleukin 8. Br J Cancer 86: 301-308, 2002.
52. Korbecki J, Kojder K, Kapczuk P, Kupnicka P, Gawrońska-Szklarz B, Gutowska I, Chlubek D and Baranowska-Bosiacka I: The effect of hypoxia on the expression of CXC chemokines and CXC chemokine receptors-a review of literature. Int J Mol Sci 22: 843, 2021.
53. Chang MM, Harper R, Hyde DM and Wu R: A novel mechanism of retinoic acid-enhanced interleukin-8 gene expression in airway epithelium. Am J Respir Cell Mol Biol 22: 502-510, 2000.
54. Mukherjee S, Date A, Patravale V, Korting HC, Roeder A and Weindl G: Retinoids in the treatment of skin aging: An overview of clinical efficacy and safety. Clin Interv Aging 1: 327-348, 2006.
55. Duong V and Rochette-Egly C: The molecular physiology of nuclear retinoic acid receptors. from health to disease. Biochim Biophys Acta 1812: 1023-1031, 2011.
56. Dai X, Yamasaki K, Shirakata Y, Sayama K and Hashimoto K: All-trans-retinoic acid induces interleukin-8 via the nuclear factor-KappaB and P38 mitogen-activated protein kinase pathways in normal human keratinocytes. J Invest Dermatol 123: 1078-1085, 2004.
57. Hoffmann E, Dittrich-Breiholz O, Holtmann H and Kracht M: Multiple control of interleukin-8 gene expression. J Leukoc Biol 72: 847-855, 2002.
58. Kunsch C, Lang RK, Rosen CA and Shannon MF: Synergistic transcriptional activation of the IL-8 gene by NF-Kappa B P65 (RelA) and NF-IL-6. J Immunol 153: 153-164, 1994.
59. Kunsch C and Rosen CA: NF-Kappa B subunit-specific regulation of the interleukin-8 promoter. Mol Cell Biol 13: 6137-6146, 1993.
60. Harant H, de Martin R, Andrew PJ, Foglar E, Dittrich C and Lindley IJ: Synergistic activation of interleukin-8 gene transcription by all-trans-retinoic acid and tumor necrosis factor-alpha involves the transcription factor NF-KappaB. J Biol Chem 271: 26954-26961, 1996.
61. Jambrovics K, Uray IP, Keresztessy Z, Keillor JW, Fésüs L and Balajthy Z: Transglutaminase 2 programs differentiating acute promyelocytic leukemia cells in all-trans retinoic acid treatment to inflammatory stage through NF-KB activation. Haematologica 104: 505-515, 2019.
62. Alfaro C, Sanmamed MF, Rodríguez-Ruiz ME, Teijeira Á, Oñate C, González Á, Ponz M, Schalper KA, Pérez-Gracia JL and Melero I: Interleukin-8 in cancer pathogenesis, treatment and follow-up. Cancer Treat Rev 60: 24-31, 2017.
63. Yuan A, Chen JJW, Yao PL and Yang PC: The role of interleukin-8 in cancer cells and microenvironment interaction. Front Biosci 10: 853-865, 2005.
64. Singh S, Wu S, Varney M, Singh AP and Singh RK: CXCR1 and CXCR2 silencing modulates CXCL8-dependent endothelial cell proliferation, migration and capillary-like structure formation. Microvasc Res 82: 318-325, 2011.
65. Waugh DJJ and Wilson C: The interleukin-8 pathway in cancer. Clin Cancer Res 14: 6735-6741, 2008.
66. Wang H, Tian Y, Wang J, Phillips KLE, Binch ALA, Dunn S, Cross A, Chiverton N, Zheng Z, Shapiro IM, *et al*: Inflammatory cytokines induce NOTCH signaling in nucleus pulposus cells. J Biol Chem 288: 16761-16774, 2013.
67. Siekmann AF and Lawson ND: Notch signalling and the regulation of angiogenesis. Cell Adh Migr 1: 104-106, 2007.
68. Benedito R, Roca C, Sörensen I, Adams S, Gossler A, Fruttiger M and Adams RH: The notch ligands Dll4 and jagged1 have opposing effects on angiogenesis. Cell 137: 1124-1135, 2009.

69. Akil A, Gutiérrez-García AK, Guenter R, Rose JB, Beck AW, Chen H and Ren B: Notch signaling in vascular endothelial cells, angiogenesis, and tumor progression: An update and prospective. Front Cell Dev Biol 9: 642352, 2021.
70. Petreaca ML, Yao M, Liu Y, Defea K and Martins-Green M: Transactivation of vascular endothelial growth factor receptor-2 by interleukin-8 (IL-8/CXCL8) is required for IL-8/CXCL8-induced endothelial permeability. Mol Biol Cell 18: 5014-5023, 2007.
71. Martin D, Galisteo R and Gutkind JS: CXCL8/IL8 stimulates vascular endothelial growth factor (VEGF) expression and the autocrine activation of VEGFR2 in endothelial cells by activating NFkappaB through the CBM (Carma3/Bcl10/Malt1) complex. J Biol Chem 284: 6038-6042, 2009.
72. Yang L, Shi P, Zhao G, Xu J, Peng W, Zhang J, Zhang G, Wang X, Dong Z, Chen F and Cui H: Targeting cancer stem cell pathways for cancer therapy. Signal Transduct Target Ther 5: 8, 2020.
73. Ciccone V, Morbidelli L, Ziche M and Donnini S: How to conjugate the stemness marker ALDH1A1 with tumor angiogenesis, progression, and drug resistance. Cancer Drug Resistance 3: 26-37, 2020.